Molecular Characterization of ADP-ribosyl Cyclase Coupled with Receptors

受容体とカップルするADPリボシールシクラーゼ分子の個体レベルでの解析

（課題番号　12480228）

平成12年度～平成14年度科学研究費補助金

基盤研究B(2)研究成果報告書

平成 15 年 5 月

研究代表者　　東田陽博

（金沢大学大学院医学系研究科・教授）

目　　次

1．はしがき

2．研究組織

3．研究経費

4．研究発表（1）学会誌等
　　（2）口頭発表
　　（3）著書

5．研究成果（日本語版）

6．研究成果（英語版）

7．謝辞と展望

8．添付　　学会誌での発表原著
　　学会誌等での発表
　　出版物（著書）

1．はしがき

私達は 10 数年来、受容体からイオンチャネルに至るシグナル伝達について研究している。ことにムスカリン性アセチルコリンやブラジキニン両受容体刺激により、イオンコンダクタンスを減少させ膜を興奮させる M タイプのカリウム（K^+）イオンチャネルに興味を持っている。M と K^+チャネルの遺伝子が KCNQ チャネルであることがわかり、サイクリック ADP リボース（cADPR）とプロテインキナーゼ C が M KCNQ チャネル抑制のセカンドメッセンジャーではないかという仮定のもとに研究を進めてきた。

後者の成果として KCNQ を抑制するプロティンキナーゼは AKAP (A Kinase anchoring protein)と結合する C－キナーゼであることを見い出し、この 6 月に Nautre Neuroscience に発表する。また、cADPR 産生酵素（ADP-ribosyl cyclase）活性を持つリンパ球細胞膜表面抗原であるヒト CD38 cDNA の大量発現細胞を作り、cADPR の細胞内作用を研究しているうちに、思いがけなく、内在性の ADP-ribosyl cyclase がムスカリン受容体により、G タンパク質を介してその活性を上下させることを知った。この情報交換機構は、非骨格筋細胞内でリアノジン受容体の関与する。即ち、Ca^{2+} induced Ca^{2+}-release 機構の関与する Ca^{2+}バイオシグナル分野で長らく疑問とされていた宿題に対する一つの回答であった。

そこで我々は、（非骨格筋細胞に存在する II 型の）リアノジン受容体に作用する cADPR の産生機構の分子機構解明を目指し、平成 9 ～11 年度に「脳型 ADP リボシルシクラーゼの精製と cDNA クローニング」という課題の研究補助を受け、研究をスタートさせた。また、12 年度から 3 年間にわたり、「受容体とカップルする ADP リボシルシクラーゼ分子の個体レベルでの解析」という課題で研究を深化させた。

その結果①ラット心臓心室筋細胞での ADP リボシルシクラーゼがβ受容体により活性化されること、②培養脳アストロ細胞で ADP リボシルシクラーゼがβ受容体により活性化されること、③神経腫瘍細胞 NG108-15 細胞に注入した cADPR により、L 型 Ca チャネルが活性化されること、④生後 1 週間以内の心筋では、アンギオテンシン受容体と ADP リボシルシクラーゼがカップルしていること、⑤代謝型グルタミン酸受容体はサブタイプ特異的にカップルすること、⑥上頚神経節細胞のムスカリン受容体が ADP リボシルシクラーゼとカップルし、cADPR が M チャネル抑制の感受性」を規定していることなどを CD38 ノックアウトマウスを使い証明した。

以上、ADP リボシルシクラーゼの遺伝子から細胞や個体レベルでの解析を行い成果をあげた。

2．研究組織

研究代表者：東田陽博（金沢大学大学院医学系研究科・教授）

研究分担者：横山　茂　（金沢大学大学院医学系研究科・助教授）

※平成 12，13 年度のみ
研究分担者：橋井美奈子（金沢大学大学院医学系研究科・講師）
研究分担者：星　直人　（金沢大学大学院医学系研究科・助手）

3．研究経費

交付決定額（配分額）

	直接経費	間接経費	合計
平成 12 年度	5,300,000	0	5,300,000
平成 13 年度	3,600,000	0	3,600,000
平成 14 年度	4,300,000	0	4,300,000
総計	13,200,000	0	13,200,000

4．研究発表

(1) 学会誌等

（和文）

東田陽博，横山　茂，木村康宏，武田　久，橋井美奈子，星　直人，高橋博人，申　然淑，張　家生，陳　小良，大巻深穂，武藤　恵，野田百美，金中　振国，Alla Egorova：血漿キニンの受容体と細胞内情報伝達の分子生物学
特集—カリクレイン・キニン系の最近の進歩—
血管と内皮　Vol. 10:　9-13, 2000.　メディカルビュー社

（英文）

Higashida, Haruhiro, Brown, David A. and Robbins, Jon:　Both linopirdine- and WAY123,398-sensitive components of IK(M,ng) are modulated by cyclic ADP ribose in NG108-15 cells.
Pflgers Archiv. Eur. J. Physiol.　441:　228-234, 2000.

Higashida, Haruhiro, Zhang, Jia-Sheng, Hashii, Minako, Shintaku Miyuki, Higashida, Chiharu and Takeda, Yoshiyu:　Angiotensin II stimulates cyclic

ADP-ribose formation in neonatal rat cardiac myocytes.
Biochem. J. 352: 197-202, 2000.

Hotta, Taeko, Asai, Kiyofumi, Fujita, Kaori, Kato, Taiji and Higashida, Haruhiro: Membrane-bound form of ADP-ribosyl cyclase in rat cortical astrocytes in culture.
J. Neurochem. 74: 669-675, 2000.

Hashii, Minako, Minabe, Yoshio and Higashida, Haruhiro: Cyclic ADP-ribose potentiates Ca2+ elevation and Ca2+ entry via L-type voltage-activated Ca2+ channels in NG108-15 neuronal cells.
Biochem. J. 345: 207-215, 2000.

Higashida, Haruhiro, Hashii, Minako, Yokoyama, Shigeru, Hoshi, Naoto, Asai, Kiyofumi and Kato Taiji: Cyclic ADP-ribose as a potential second messenger for neuronal Ca2+ signaling.
J. Neurochem. 76: 321-331, 2001.

Higashida, Haruhiro, Yokoyama, Shigeru, Hoshi, Naoto, Hashii, Minako, Egorova, Alla, Zhong, Zhen-Guo, Noda, Mami, Shahidullah, Mohammad, Taketo, Megumi, Knijnik, Rimma, Kimura, Yasuhiro, Takahashi, Hiroto, Chen, Xian-Liang, Shin, Yeonsook and Zhang, Jia-Sheng: Signal transduction from bradykinin, angiotensin, adrenergic and muscarinic receptors to effector enzymes, including ADP-ribosyl cyclease.
Biological Chem. 382: 23-30, 2001.

Higashida, Haruhiro, Hashii, Minaka, Yokoyama, Shigeru, Hoshi, Naoto, Chen, Xian-Liang, Egorova, Alla, Noda, Mami and Zhang, Jia-Sheng: Cyclic ADP-ribose as a second messenger revisited from a new astherapeutics.
Pharmacol. Therapeut. 90: 283-296, 2001.

Higashida, Haruhiro, Hossain, Kazi Z., Takahagi, Hiroko and Noda, Mami: Measurement of adenylyl cyclase by separating cyclic AMP on silica gel thin-layer chromatography.
Anal. Biochem. 308: 106-111, 2002.

Noda, Mami, Yasuda, Satsuki, Okada, Mitsuko, Higashida, Haruhiro, Shimada, Aki, Iwata, Nakao, Ozaki, Norio, Nishikawa, Kaori, Shirasawa, Sakiko, Uchida, Mayumi, Aoki, Shunsuke and Wada, Keiji: Recombinant human serotonin 5A receptors stably expressed in C6 glioma cells couple to multiple signal transduction pathways.
J. Neurochem. 84: 222-232, 2003.

Higashida, Haruhiro, Zhang, Jia-Sheng, Mochida, Sumiko, Chen, Xiao-Liang, Shin, Yeonsook, Noda, Mami, Hossain, Kazi Z., Hoshi, Naoto, Hashii, Minako, Shigemoto, Ryuuichi, Nakanishi, Shigetade, Fukuda, Yutaka and Yokoyama, Shigeru: Subtype-specific coupling with ADP-ribosyl cyclase of metabotropic glutamate receptors in retina, cervical superior ganglion and NG108-15 cells.

J. Neurochem. in press.

Hoshi, Naoto, Zhang, Jia-Sheng, Omaki, Miho, Takeuchi, Takahiro, Yokoyama, Shigeru, Wanaverbecq, Nicolas, Langeberg, Lorene K., Yoneda, Yukio, Scott, John D., Brown, David A. and Higashida, Haruhiro: AKAP150 signaling complex promotes suppression of the M-current by muscarinic agonists.

Nature Neurosci. in press.

(2) 口頭発表

東田陽博：サイクリック ADP リボース産成からみた心収縮のメカニズム

第 78 回日本生理学大会 (2001. 3. 29-31) (京都)

Higashida, H., Egorova, A., Higashida, C., Zhong, Z.-G., Yokoyama, S., Noda, M.and Zhang, J.-S.: Increased cADP-ribose synthesis by activation of adrenergic receptors with norepinephrine in ventricular muscle cell membranes is involved in upregulation of cardiac function by sympathetic stimulation.

9th International Catecholamine Symposium. (2001. 3. 30- 4. 5) (京都)

Higashida, H., Zhang, J.-S., Hashii, M., Shintaku, M., Higashida, C. and Taakeda, Y.:
Angiotensin II stimulates cyclic ADP-ribose formation in neonatal rat cardiac myocytes.

The Third Japan-Korea Joint Symposium of Brain Sciences, and Cardiac and Smooth Muscles. (第 3 回日韓脳科学・心筋・平滑筋シンポジウム) (2002. 1. 18-20) (久留米)

東田陽博、横山 茂、陳 小良、張 家生、星 直人、橋井美奈子：神経細胞でサイクリック ADP リボースは真のセカンドメッセンジャーであるか

第 20 回放射性同位元素研究連絡会 (2002. 3. 19) (金沢)

陳 小良、東田陽博：Neuronal Calcium sensor-1/Frequenin の大量発現によるアセチルコリン遊離増強

第 79 回日本生理学会大会ワークショップ「シナプス機能とカルシウム」

（2002. 3. 28-30）（広島）

東田陽博、陳　小良、張　家生、野田百美、星　直人、橋井美奈子、横山　茂：網膜内グループ III グルタメート受容体の ADP リボシールシクラーゼへのカップリング

第 45 回日本神経化学会（札幌）大会（2002. 7. 16-19）（札幌）

Zhang, J.-S., Higashida, H.: Acetylcholine stimulates cyclic ADP-ribose formation via muscarinic receptors in rat superior cervical ganglion (SCG)

第 75 回日本生化学会大会 （2002. 10. 14-17）（京都）

東田陽博：神経科学の新しい解析法とその応用

生理学研究所研究会（2002. 11. 14-16）（岡崎）

東田陽博：Possiblesecond messengers and intracellular signal transduction mechanism for acetylcholine-induced M-current inhibition in neurons.

日米科学技術協力事業「脳研究」分野情報交換セミナー「Neural Signalplexes and Ion Channel Regulation」（2003. 3. 16-18）（岡崎）

東田陽博、星　直人：Possiblesecond messengers and intracellular signal transduction mechanism for acetylcholine-induced M-current inhibition in neurons.（アセチルコリンによるM電流抑制を生じるセカンドメッセンジャーと信号伝達機構）

第 80 回日本生理学会大会「KCNQ タイプKチャネルと抗痴呆・てんかん薬」シンポジウム（2003. 3. 23-26）（福岡）

(3) 著書

（和文）

野田百美、安田さつき、東田陽博、和田圭司：セロトニン 5A 受容体とグリア細胞：その機能と病態について

脳機能の解明－生命科学の主潮流－　p179-184, 2002.
赤池紀扶、東　英穂、阿部康二、久保千春編　ガイア出版会
（九州大学出版会）

（英文）

Higashida, Haruhiro, Zhang, Jia-Sheng,Yokoyama, Shigeru, Noda, Mami, Zhong, Zhen-Guo, Mochida, Sumiko and Egorova, Alla: Sympathetic potentiatioin of cyclic ADP-ribose formation rat cardiac myocytes.

Catecholamine Research from Molecular Insights to Clinical Medicine
Edited by T. Nagatsu, T. Nabeshima, R. McCarty, D.S. Goldstein
Advances in Behavioral Biology. Vol 53: 73-76, 2002.

5．研究成果（日本語版）

パートI

ADPリボシルシクラーゼとカップルする代謝型グルタミン酸受容体サブタイプ

サイクリック ADP リボース（cADPR）はセカンドメッセンジャーであると考えられているが、代謝型グルタミン酸受容体（mGluR）の下流での役割はわかっていない。ラットやマウスの上頚神経節（SCG）や網膜から取った粗膜分画を酵素源として、グルタミン酸を投与すると NGD から cGDPR や［3H］cADPR の産成が増加した。薬理学的検討から SCG はグループ I 、網膜はグループ III の mGluR の関与が考えられた。mGluR 6 ノックアウトマウスの網膜ではグルタミン酸に対する反応は消失した。mgluR 1 が mGluR 7 の cDNA を NG108-15 細胞に発現し、クローン受容体レベルでADPRシクラーゼ反応を確認した。mGluR 1, 3, 5, 6 がADPRシクラーゼを上昇させ mGluR 2 は減少させた。グループ II, III の中にカップリング様式の異なるサブタイプがあることから、表に示すような新しいサブタイプ分類を提唱した。

Subclassification of mGluRs according to coupling preference and localization in synaptic regions.

Group	Subtype	Coupling to			Synaptic localization*	
		NC**	AC**	PLC**	Presynaptic	Postsynaptic
I a	mGluR1	↑	↑	↑	-	Peri, Extra
I a	mGluR5	↑	↑	↑	-	Peri, Extra
II a	mGluR3 ↑	↓			Extra	PSD, Peri, Extra
II b	mGluR2 ↓	↓			Extra	Extra
III a	mGluR6 ↑	↓		-		BCE
III c	mGluR4 →	↓			Active zone	-
III c	mGluR7 →	↓			Active zone	-

*Based upon observations described in the text. Peri, perisynaptic site; Extra, extrasynaptic site; PSD, postsynaptic density; BCE, base of central element; -, not detected.

**NC, ADP-ribosyl cyclase; AC, adenylyl cyclase; PLC, phospholipase C. ↑, activation; ↓, inhibition; →, no effect.

パートII

アセチルコリンによるM電流抑制をCD38/ADPリボシルシクラーゼの遺伝子的変異により変化させた

ムスカリン性アセチルコリン受容体（mAchR）によるM電流抑制におけるADPリボシルシクラーゼ/CD38の役割を検討した。上頚神経節（SCG）の膜分画にアセチルコリンを投与するとADPリボシルシクラーゼが濃度依存的に上昇した。ADPRが産生されないCD38ノックアウトマウスノSSCGではアセチルコリン投与では上昇しなかった。また、M電流も正常ネズミのSCG神経細胞と同じ電位量であったが、アセチルコリン投与によりM電流は25%しか減少しなかった（正常ネズミでは75%）。一方CD38をNG108-15細胞に大量発現したNG108-15細胞では、逆にM電流減少が3倍以上増大した（下図C参照）。

以上の結果よりcADPRよりM電流チャネルへの信号伝達を変化させることがわかった。

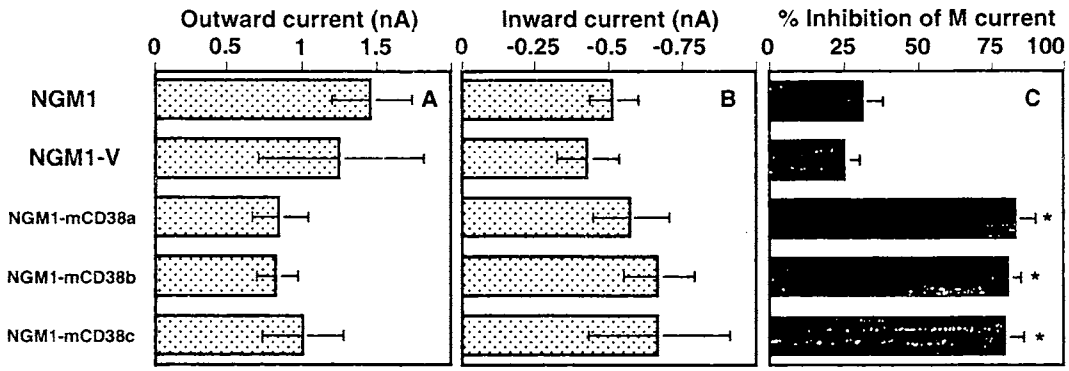

6. 研究成果　（英語版）

Part I

Subtype-specific coupling with ADP-ribosyl cyclase of metabotropic glutamate receptors in retina, cervical superior ganglion and NG108-15 cells

Running title: Selective coupling of mGluRs with ADP-ribosyl cyclase

Abstract

Cyclic ADP-ribose (cADP-ribose) is a putative second messenger or modulator. However, the role of cADP-ribose in the downstream signals of the metabotropic glutamate receptors (mGluRs) is unclear. Here, we show that glutamate stimulates ADP-ribosyl cyclase activity in rat or mouse crude membranes of retina via group III mGluRs or in superior cervical ganglion via group I mGluRs. The retina of mGluR6 deficient mice showed no increase in the ADP-ribosyl cyclase level in response to glutamate. GTP enhanced the initial rate of basal and glutamate-stimulated cyclase activity. GTP-γ-S also stimulated basal activity. To determine whether the coupling mode of mGluRs to ADP-ribosyl cyclase is a feature common to individual cloned mGluRs, we expressed each mGluR subtype in NG108-15 neuroblastoma x glioma hybrid cells. The glutamate-induced stimulation of the cyclase occurs preferentially in NG108-15 cells over-expressing mGluRs1, 3, 5, and 6. Cells expressing mGluR2 or mGluRs4 and 7 exhibit inhibition or no coupling, respectively. Glutamate-induced activation or inhibition of the cyclase activity was eliminated after pretreatment with cholera or pertussis toxin, respectively. Thus, the subtype-specific coupling of mGluRs to ADP-ribosyl cyclase via G

proteins suggests that some glutamate-evoked neuronal functions are mediated by cADP-ribose.

Keywords: cyclic ADP-ribose, second messengers, glutamate, signal transduction

Introduction

Metabotropic glutamate receptors (mGluRs) are coupled to G proteins and evoke a variety of neuronal functions, such as modulation of membrane currents, neurotransmitter release, plasticity, cortical differentiation, and addiction, by mediating intracellular signal transduction (Nakanishi, 1992 and 1994; Conn and Pin, 1997; Nakanishi et al., 1998; Chiamulera et al., 2001; Hannan et al., 2001; Miura et al., 2002). There are eight genetically-different subtypes designated mGluR1 to mGluR8 (Nakanishi, 1992 and 1994; Duvoisin et al., 1995). On the basis of their sequence similarity and pharmacology, mGluRs have been defined to belong to three distinct groups (groups I, II and III) (Nakanishi, 1992; Conn and Pin, 1997). However, from the view point of signal transduction, the mGluR subtypes can be largely divided into two classes: those that couple to phospholipase C and/or D (group I, mGluRs1 and 5) (Nakanishi, 1994; Nakanishi e al., 1998; Servitja et al., 1999), and those that negatively regulate adenylyl cyclase (group II, mGluRs2 and 3, and group III, mGluRs4, 6-8) (Nakanishi, 1992; Tanabe et al., 1992; Nakajima et al., 1993; Okamoto et al., 1994; Duvoisin et al., 1995). In contrast, recent in situ hybridization and immunohistological studies have revealed that the mGluR subtypes display diverse but distinct distribution in brain regions and more complex pre- and post-synaptic localizations (Masu et al., 1991; Tanabe et al., 1992; Abe et al., 1992; Nomura et al., 1994; Ottersen and Landsend, 1997; Shigemoto et al., 1997; Cartmell and Schoepp, 2000; Neto et al., 2000; Tamaru et al., 2001). Collectively, these results indicate that multiple intracellular signal pathways may exist for different mGluR subtypes to play numerous roles in neuronal function.

In mGluR-mediated Ca^{2+} signaling, group I mGluRs can increase intracellular Ca^{2+} concentrations in brain neurons by Ca^{2+} mobilization from inositol-1,4,5-trisphosphate-sensitive Ca^{2+} stores, interacting with Homer proteins between them (Nakanishi, 1992 and 1994; Crawford et al., 2000; Fagni et al., 2000; Ango et al., 2001; Morikawa et al., 2003). In addition, activation of group I mGluRs mediates increased Ca^{2+} entry through L- or N-type Ca^{2+} channels (Anwyl, 1999), especially in a ryanodine receptor-dependent manner (Chavis

et al., 1996). Although mGluRs sometimes cause inhibition of voltage–dependent Ca^{2+} channels (Ikeda et al., 1995; Anwyl, 1999), these mGluR-mediated Ca^{2+} elevations can often activate Ca^{2+}-dependent K^+ or non-selective cationic channels (Pollock et al., 1999; Fagni et al., 2000; Morikawa et al., 2003). In retina, depolarization of 'ON' bipolar cells is thought to be mediated by the inactivation of mGluR6 with light (Nawy, 2000), and increases conductance of cyclic GMP-dependent cation channels accompanied by subsequent Ca^{2+} concentration elevations (Shiells and Falk, 1999). However, little is known about how mGluRs interact with the Ca^{2+} amplification machinery, namely functional triads consisting of ryanodine receptors, Ca^{2+} channels, and Ca^{2+}-activated K^+ channels (Akita and Kuba, 2000).

One possibility is the involvement of cyclic ADP-ribose (cADP-ribose), a putative second messenger (Lee, 2001; Higashida et al., 2001). cADP-ribose potentiates Ca^{2+}-induced Ca^{2+}-release at neuronal ryanodine receptors triggered by Ca^{2+} influx, designated an 'orthograde signal' (Empson and Galione, 1997; Pollock et al., 1999; Hashii et al., 2000). Subsequently, increased Ca^{2+} affects Ca^{2+} channels indirectly through ryanodine receptors activated by cADP-ribose, referred to as a 'retrograde signal' (Chavis et al.,1996; Empson and Galione, 1997; Hashii et al., 2000). Therefore, our favored hypothesis is that cADP-ribose plays a role as a soluble factor for mGluR-mediated Ca^{2+} signaling.

We previously reported that stimulation of β-adrenergic and angiotensin II receptors modulates activity of ADP-ribosyl cyclase, a synthetic enzyme of cADP-ribose, and showed that cADP-ribose is a critical molecule in sympathetic potentiation of heart contraction, post-natal heart growth, and neuron-glia interaction (Higashida et al., 1999 and 2001). In the present study, we used the same strategy to explore the idea that cADP-ribose is a second messenger downstream of the mGluRs. We first measured ADP-ribosyl cyclase activity in crude membranes from various rat and mouse nervous tissues in the presence or absence of glutamate and/or GTP. Second, the coupling preference of mGluRs to ADP-ribosyl cyclase was examined in NG108-15 neuroblastoma x glioma hybrid cells over-expressing each

subtype.

Materials and methods

Membrane preparation

Wistar rats (1 to 12 weeks old) and adult wild-type or mGluR6$^{-/-}$ mice (Sugihara et al., 1997) were anesthetized using diethylether and decapitated. Various brain regions, retina and superior cervical ganglion (SCG) were isolated and minced, and NG108-15 cells frozen at –80 °C were thawed. Nervous tissues or cells were then suspended in a hypotonic solution (10 mM Tris-HCl solution, pH 7.3, with 5 mM $MgCl_2$) at 4°C for 30 min. The cell suspensions were homogenized in a glass homogenizer, and the resultant homogenate was centrifuged at 4°C for 5 min at 1000 x g to remove unbroken cells and nuclei. Crude membrane fractions were prepared by centrifugation (twice) of homogenates at 105000 x g for 15 min. The supernatant was removed and the pellet was washed twice, the final pellet was dispersed in 10 mM Tris-HCl solution, pH 6.9, and used immediately for enzymatic reactions. In some experiments, NG108-15 cells were treated with chorela toxin (CTx) or pertussis toxin (PTx) (100 ng/ml) for 8-16 h in culture dishes. Rats were intraperitoneally injected with CTx (100 ng per g of body weight) 16 h before sacrifice.

ADP-ribosyl cyclase and cADP-ribose hydrolase assay

Cell membranes (1.2-6 μg), prepared as above, where placed in 20 μl of reaction mixture containing Tris-HCl (50 mM, pH 7.1), 100 mM KCl, 5 mM $MgCl_2$, 0.1 mM EDTA, 2 μMNAD$^+$, [^{3}H] β-NAD$^+$ (0.11 μM, 0.06 μCi) with or without glutamate and GTP slightly modified to what was reported previously (Higashida et al., 1997 and 1999). Reaction mixtures were incubated for 2 min at 37 °C and stopped by the addition of 2 μl trichloroacetic acid (15%). Aliquots were centrifuged (14000 x g, 2.5 min) and 2 μl of the

supernatant was spotted on silica gel plastic thin layer chromatography sheets (20 x 10 cm). The layer was developed in the ascending direction for 40-60 min at room temperature in a mixture consisting of 30% water, 70% ethanol and 0.2 M ammonium bicarbonate (Higashida et al., 1997 and 2002). The positions of authentic cADP-ribose, ADPR and β-NAD^+ after UV detection were detected and confirmed by autoradiogram of TLC with [^{3}H]β-NAD^+ obtained after exposure (24 - 36 hours) on a [^{3}H] imaging plate (Fuji BAS 1000, Tokyo, Japan) in each run. Corresponding positions on the experimental runs were cut out of the gel (about 1 cm by 0.7 cm) and the radioactivity counted in a liquid scintillation counter. cADP-ribose hydrolase activities were also assayed in 20-μl reaction mixtures contained 2 μM [^{3}H]cADP-ribose (0.015 μCi), according to a previously described formula (Higashida et al., 1997).

Fluorometrical measurement of ADP-ribosyl cyclase

ADP-ribosyl cyclase activity was determined fluorometrically using a technique based on the measurement of the conversion of β-nicotinamide guanine dinucleotide$^+$ (β-NGD^+) into the fluorescent product cyclic GDP-ribose (cGDP-ribose), as described previously (Graeff et al., 1994; Higashida et al., 1999). Briefly, 2.4 ml of reaction mixtures containing 60 μM β-NGD^+, 50 mM Tris-HCl, pH 6.9,. 100 mM KCl, 10 μM $CaCl_2$ and membranes (1.5-55.4 μg of protein) were maintained at 37°C with constant stirring. The samples were then excited at 300 nm and fluorescence emission was continuously monitored at 410 nm in a Shimadzu RF-5300PC spectrofluorophotometer (Kyoto, Japan). Enzyme activity was determined as the slope of curves computed from data points obtained every 60 ms, and confirmed by curve fitting of smoothing-processed data.

Electrophysiological measurements

Collagenased rat SCG cells were cultured and membrane potentials of ganglion neurons were recorded with a sharp intracellular microelectrode, as previously described (Mochida et al., 1994).

Construction of expression plasmids

Expression plasmids carrying the entire coding sequences for the mGluRs1-7 were constructed as follows. The *Eco*RV/*Not*I fragments from pmGR1 (Masu et al., 1991) were ligated to *Not*I/*Eco*RV-cleaved pcDNA3 (Invitrogen) to obtain pcDmGR1a. The *Eco*RI fragments from pmGRs2, 3 and 4 (Tanabe et al., 1992), and pmGR6 (Nakajima et al., 1993) were cloned into the *Eco*RI sites of pcDNA3 to obtain pcDmGR2, pcDmGR3, pcDmGR4a, and pcDmGR6, respectively. The *Eco*RI/*Not*I fragments from pmGR5 (Abe et al., 1992) and pmGR7 (Okamoto et al., 1994) were ligated to *Not*I/*Eco*RI-cleaved pcDNA3 to yield pcDmGR5a and pcDmGR7a.

Transient or stable transfection of mGluR cDNAs into NG108-15 cells

Mouse neuroblastoma x rat glioma hybrid NG108-15 cells (5 x10^5) were plated in 60-mm dishes (Higashida et al., 1997). Twenty-four h later, the cells were transfected with 10 μg each of pcDmGR1a-7a or pcDNA3 mixed with 25 μl Lipofectamine plus (Gibco-BRL). The transfection efficiency of pcDNA3 was 15-35% (n=5) in NG108-15 cells in dishes transfected with pcDNA3 inserted with neuronal calcium sensor 1 fused with green fluorescence protein, according to results from the fluorescence-positive cells. One day after transfection, harvested cells were further cultured in new 60-mm dishes for 4 days for the ADP-ribosyl cyclase assay. Some cells were characterized by Western blotting using six monoclonal or polyclonal antibodies (A52, mG2Na-5, Y33, K44, G53, and G74) which recognize mGluRs1a, 2, 3, 4a, 5, and 7a and an antiserum against mGluR6 (Shigemoto et al., 1997; Tamaru et al., 2001).

Stable NG108-15 clones over-expressing each mGluR were generated by transfecting the cells with pcDmGRs1-7 and selecting in 800 μg/ml geneticin. At least two clones of transfectants expressing each mGluR subtype were selected, and characterized by Western blotting and measurement of adenylyl cyclase. Adenylyl cyclase activity was measured in a

100 μl reaction mixture containing 0.32 mM [^{32}P]ATP (0.6 μCi), and [^{32}P]cAMP was separated with thin-layer chromatography by using the same solvent for separating cADP-ribose as described previously (Higashida et al., 2002).

Statistical analysis

All values are represented as mean ± S.E.M. Homogeneity of variance was tested with Fischer's *F* test followed by Student' *t* test using two-way analysis of homogeneous variance.

Results

ADP-ribosyl cyclase activity was measured using radioisotopes (Higashida et al., 1997) or by the formation rate of nonhydrolyzable cGDP-ribose from β-NGD$^+$ (Graeff et al., 1994; Higashida et al., 1999) with crude membranes isolated from various regions of the nervous system. ADP-ribosyl cyclase activity was detected in the olfactory bulb, cerebral cortex, hippocampus, cerebellum, retina or SCG of 1- to 12-week-old rats. [^{3}H]cADP-ribose formation and cGDP-ribose fluorescence increased upon exposure to glutamate (100 nM and 1 μM) in crude membrane fractions of both retina and SCG in the presence of endogenous GTP (Figs. 1 and 2), but was not much influenced in other brain regions, including in the olfactory bulb, cerebral cortex, hippocampus, cerebellum. The mean ADP-ribosyl cyclase activity was 49.3 ± 23.6 and 495.5 ± 226.9 pmol/min/mg of protein (n=4) for retina and SCG of 4-week-old rats, respectively. Total activities of ADP-ribosyl cyclase were about 0.86 pmol/min/SCG and 0.38 pmol/min/retina in 4-week-old rats, respectively. The increase in [^{3}H]cADP-ribose formation induced by 10 μM glutamate was 188.3 ± 46.1% in retina and 195.0 ± 36.4% in SCG (n=4; vs. no glutamate, $p < 0.05$; Fig. 1), respectively. Differing from the responses in the rat heart to angiotensin II and isoproterenol (Higashida et al., 2001), coupling efficiency and preference of ADP-ribosyl cyclase to glutamate was not much changed developmentally in retina and SCG of 2-4-weeks old to young adult rats.

In contrast, cADP-ribose hydrolase activity was barely detectable in both retina and

SCG membranes, similar to NG108-15 cells (Higashida et al., 1997). The conversion ratio to [^{3}H]ADP-ribose from [^{3}H]cADP-ribose was unchanged in the absence or presence of 10 μM glutamate. This implies that the glutamate-induced accumulation of cADP-ribose in the membranes of both retina and SCG is due to accelerated production, rather than breakdown inhibition. These findings were further studied by measuring ADP-ribosyl cyclase fluorometrically.

Glutamate-induced activation of ADP-ribosyl cyclase in retina

The increase in ADP-ribosyl cyclase was dose-dependent (Fig. 2). The increase to 205.5 ± 16.6 and 220.0 ± 20.8% (n=6 and 4) of the pre-exposure level was obtained by 1 and 10 μM glutamate in retina, respectively ($p < 0.001$). This glutamate-induced increase was mimicked by an mGluR group III-selective agonist, L(+)-2-amino-4-phosphonobutyric acid (L-AP4), but not by (S)-3,5-dihydroxyphenylglycine (DHPG) or (2S,2'R,3'R)-2-(2',3'-dicarboxycyclopropyl)glycine (DCG-IV), group I- and II-selective agonists (Fig. 3A). Exposure to 10 μM L-AP4 increased the ADP-ribosyl cyclase level to 196.1 ± 8.8% (n=6) of the control level ($p < 0.001$). An increase obtained by the glutamate (10 nM) exposure subsequent to the initial application of 10 nM L-AP4 was small, but much higher by DHPG and DCG-IV (Table 1).

In the presence of 10 μM (RS)-α-cyclopropyl-4-phosphonophenylglycine (CPPG), a group III-selective antagonist, an application of glutamate had no effect (Table 2). In contrast, application of group I- and II-selective antagonists, (RS)-1-aminoindan-1,5-dicarboxylic acid (AIDA) and (2S)-α-ethylglutamic acid (EGLU), did not lead to an increase in the ADP-ribosyl cyclase level by themselves, but subsequent glutamate (10 nM - 1 μM) did, suggesting that this glutamate effect in retina is mediated via the group III mGluRs.

The most abundant subtype in retina is mGluR6 (Nakajima et al., 1993), though other mGluR subtypes are also expressed (Duvoisin et al., 1995; Hartveit et al., 1995). To define whether mGluR6 mediates ADP-ribosyl cyclase activation, we used mGluR6 deficient mice

(Sugihara et al., 1997). The mGluR6$^{-/-}$ retina showed no increase in the ADP-ribosyl cyclase level in response to 1 μM glutamate (101.9 ± 5.7%, n=7, vs. no glutamate, Fig. 4A), while the retina from wild-type mice showed an identical increase to the rat retina (201.0 ± 20.4%, n=6; P<0.001 vs. mGluR6$^{-/-}$). In the control experiment, glutamate increased ADP-ribosyl cyclase activity in the SCG of both mGluR6$^{+/+}$ and mGluR6$^{-/-}$ mice equally (Fig. 4B). These results indicate that retinal activation is primarily due to mGluR6, while that of SCG is due to other mGluR subtypes.

In separate experiments, optimal conditions for the assay and effects of glutamate were examined in more detail with retinal preparations. Production of cGDP-ribose was optimal at about pH 6.5 (at 37 °C), similarly shown in ADP-ribosyl cyclase activity of cardiac myocytes (Higashida et al., 1999). However, the glutamate-induced activation was obtained only at the more alkaline range than 6.8 (data not shown). Thus, it is confirmed that the identical activation (up to 2- to 3-fold) by glutamate was observed at the physiological pH range, though the basal activity was reduced.

Glutamate-induced activation of ADP-ribosyl cyclase in SCG

The maximum increase in ADP-ribosyl cyclase to 201.3 ± 17.9% (n=7) and 194.7 ± 10.8% (n=3) of the pre-exposure level was obtained by 1 or 10 μM glutamate in the SCG (Fig 2; P<0.001). Unlike retina, this glutamate-induced increase was mimicked by DHPG (1 μM, 198.7 ± 15.5%, n=3; P<0.01), but not by DCG-IV or L-AP4 (Fig. 3B). Glutamate induced a further activation even after the treatment with DCG-IV or L-AP4, but not with DHPG (Table 1). In the presence of 10 μM AIDA, but not EGLU or CPPG, glutamate (10 nM) failed to induce an increase in the ADP-ribosyl cyclase level (Table 2). These results suggest that, pharmacologically, the effect of glutamate in the SCG is mediated via the group I mGluRs.

Despite a lack of mGluR responses in adult rat SCG (Ikeda et al., 1995), mobilization of intracellular Ca^{2+} by mGluR5 has been shown in neonatal rat dorsal root ganglion neurons in culture (Crawford et al., 2000). Therefore, we dissected SCG neurons from 10-day-old rats

and cultured them for 5-6 weeks (Mochida et al., 1994), to evaluate functional mGluRs. Application of 300 μM glutamate to cultured SCG neurons resulted in a rapid depolarization (time to peak, ~15 s) with a mean amplitude of 3.1 ± 0.84 mV (n=5), followed by a small depolarization of 0.97 ± 0.09 mV (n=5) which lasted for up to 30 min (Fig. 5). This slow depolarization was associated with an increased membrane resistance and action potential firings (data not shown), similar to group I agonist-induced depolarizing responses in enteric neurons (Liu and Kirchgessner, 2000). Exposure of neurons to glutamate also elicited a frequency increase in spontaneous excitatory postsynaptic potentials in our records (data not shown), due to an enhanced release of acetylcholine from paired SCG neurons (Mochida et al., 1994). The depolarization was mimicked by 1.5 μM DHPG (1.40 ± 0.34 mV, n=8) and significantly antagonized by 100 μM AIDA (0.13 ± 0.06 mV, n=5; $p<0.001$), indicating that cultured SCG neurons possess group I mGluRs.

Effects of GTP or GTP analogs on ADP-ribosyl cyclase activity

The above stimulation induced by glutamate seems to be due to endogenous GTP and GTP-binding proteins in membranes. Therefore, we determined whether or not mGluR-mediated activation of ADP-ribosyl cyclase in retina and SCG is reproduced by GTP and its analogue. Addition of GTP resulted in an increase in enzyme activity in retina (Fig. 6A) and SCG (Fig. 6B). A relatively symmetrical biphasic (activating and inhibitory) relationship is apparent between the concentration (0.1 nM-100 μM) of GTP, as shown in the fat cell adenylyl cyclase system by Rodbell and his colleagues (Cooper et al., 1979). GTP was more potent than glutamate in terms of its effective concentration (less than micromolar) range. GTP (100 or 10 nM) stimulated basal activity by 84.2 ± 11.4% (n=6) in retina and 109.6 ± 18.3% (n=6) in SCG ($p<0.001$).

Next, we examined the effect of glutamate in the presence of various concentrations of GTP. GTP caused a 1.5- to 2.5-fold stimulation of the response of the enzyme system to 10 nM glutamate (Fig. 6C). The maximum increase in the presence of glutamate was 271.2 ±

22.9% (n=6) at 1 μM GTP in retina or 341.8 ± 41.4% (n=4) at 10 nM GTP in SCG, respectively ($p < 0.001$).

The effect of a non-hydrolyzable analogue of GTP, GTP-γ-S, that persistently activates GTP-binding proteins, was examined. GTP-γ-S produced only an increase in cGDP-ribose forming activity in both retina and SCG. The dependency on the concentration is not bell shaped (data not shown). Increases to 207.7 ± 3.3% (n=6) in retina and 199.3 ± 6.0% (n=3) in SCG of the control were produced at 1 μM or 100 nM GTP-γ-S ($p < 0.001$), respectively. Addition of 1 μM GDP-β-S increased the cyclase activity slightly (about 10%), but blocked further increases by 1 μM glutamate in retina and SCG (n=4).

Effect of glutamate and bacterial toxin on [^{3}H]cADP-ribose formation

Glutamate-induced activation of the cyclase activity in the crude membrane of both retina and SCG in rats was eliminated after pretreatment with 100 ng/ml CTx for 8-16 h ($p < 0.01$; Fig. 7A). This suggests the likelihood that the membrane delimited effect of glutamate is mediated via the CTx-sensitive subset of G proteins. The same line of data has been obtained in m1 and m3 muscarinic receptors in NG108-15 cells (Higashida et al., 1997) and β-adrenoceptors in cardiomyocytes and cortical astrocytes (Higashida et al., 1999 and 2001).

Cyclase activity in NG108-15 cells transiently overexpressing each mGluR subtype

To determine whether the above coupling mode of mGluRs to ADP-ribosyl cyclase is a feature common to individual cloned mGluRs, we expressed each mGluR subtype in NG108-15 neuroblastoma x glioma hybrid cells. ADP-ribosyl cyclase activity was detected in membranes prepared from NG108-15 cells transiently transfected with cDNAs of each mGluR subtype, as previously characterized (Higashida et al., 1997).

Upon application of 10 nM glutamate, ADP-ribosyl cyclase activity significantly increased in membranes prepared from NG108-15 cells expressing mGluRs1 and 5, with an average activation of 177.4 ± 18.9% (n=5) and 151.0 ± 10.9% (n=3) of the pre-application

level (Fig. 8, $p < 0.01$ and 0.05), respectively. As expected, 10 nM glutamate significantly increased ADP-ribosyl cyclase activity to 214.2 ± 41.5% (n=5) of the pre-exposure level in mGluR6 expressing cells ($p < 0.01$). Surprisingly, activation of ADP-ribosyl cyclase activity to 184.6 ± 10.7% (n=7) by glutamate was also obtained in mGluR3-transfected cells ($p < 0.01$). In the control experiments, non-transfected or mock-transfected cells did not exhibit glutamate-induced activation (101.3 to 108.1% (n=4 and 8)) of the pre-application level (Fig. 8). Thus, the values obtained in NG108-15 cells over-expressing mGluRs1, 3, 5, and 6 are significantly higher than those in wild-type and mock-transfected control cells ($p < 0.001$ or 0.05).

A decrease in ADP-ribosyl cyclase activity by 10 nM glutamate to 74.4 ± 4.3% (n=5) of the pre-application level was observed in mGluR2-transfected NG108-15 cells ($p < 0.001$; Figs. 7C and 8). No or little change in cyclase activity was obtained with glutamate in mGluR4- and mGluR7-expressing NG108-15 cells (Fig. 8). Moreover, group-selective agonists faithfully replicated the glutamate responses for different subtypes (data not shown).

To exclude dysfunctional receptor expression in NG108-15 cells, we measured adenylyl cyclase activity. Glutamate (10 μM) inhibited to 83.2 ± 6.7% (n=11, $p < 0.05$) of the non-treated level in 10 μM forskolin-activated adenylyl cyclase activity in cells over-expressing mGluR4. 10 μM prostaglandin E_1-activated adenylyl cyclase activity was inhibited to 65.6 ± 6.7% (n=11, $p < 0.001$) of the non-application level in mGluR7-expressing cells. Likewise, as reported, stimulation of mGluRs2, 3 and 6 by 10 μM glutamate inhibited basal adenylyl cyclase activity to 79.4 ± 14.4% (n=5), 83.3 ± 8.1% (n=3), and 81.4 ± 12.3% (n=7) of the control, respectively ($p < 0.05$).

Signal transduction from mGluRs to ADP-ribosyl cyclase in stable clones

Finally, the coupling preferences of the mGluRs was examined in stably expressing NG108-15 cell lines. The results of stable clones matched those of transiently expressed cells, and exhibited nearly identical magnitudes of responses by 10 nM to 10 μM glutamate (Fig. 7B).

The glutamate-induced activation was blocked in mGluRs1-, 3-, and 6-expressing NG108-15 cells treated with CTx, but not with PTx. Inversely, the inhibition by glutamate in mGluR2-expressing cells was nullified with PTx (Fig. 7C).

Discussion

These results show that glutamate stimulates activity of the membrane-bound form of ADP-ribosyl cyclase in rat and mouse retina or rat SCG, and that GTP enhanced the initial rate of glutamate-stimulated activity in rat retina and SCG. This is the first biochemical demonstration of the mGluR/cADP-ribose signal transduction pathway via G proteins in the nervous system. Pharmacological effectiveness and the result obtained in mGluR6-gene-targeted mice revealed that group III (mGluR6) and group I (mGluRs1 and/or 5) mGluRs are responsible for glutamate-induced activation of ADP-ribosyl cyclase in retina and SCG, respectively. Our results of over-expression of cloned mGluRs in NG108-15 cells demonstrate subtype-specific coupling preferences of mGluRs to ADP-ribosyl cyclase, as summarized in Table 3. Cyclase activation was not only restricted to mGluRs1 and 5, but also mGluRs3 and 6. The reconstitution of mGluRs1, 5 and 6 in NG108-15 cells may represent those found in SCG and retina.

It will be interesting to show an increase of cADP-ribose concentrations by glutamate in vivo cells expressing mGluRs 1, 3, 5 and 6. However, we could not perform a kind of radioimmunoassay, because an ADPR-binding protein (antibody; Takahashi et al., 1995) was no more available. Since ryanodine receptors with a major band of 400 kd (Kuwajima et al., 1992) were detected with an anti-dog cardiac ryanodine receptor antibody in retina, SCG and NG108-15 cells in our preliminary results as shown by Ronde et al. (2000), the stimulatory mGluRs may modulate intracellular Ca^{2+} concentrations through interaction of ryanodine receptors with increased cADP-ribose. The similar evidence has recently been shown by Morikawa et al. (2003) that mGluRs can release Ca^{2+} in dopamine neurons in the

rat ventral midbrain through the activation of both inositol trisphosphate and ryanodine receptors

In the mGluRs belonging to group II, we found that inhibitory mGluR2 differs from excitatory mGluR3 with respect to glutamate-induced ADP-ribosyl cyclase activity, while both receptors equally inhibit adenylyl cyclase, as reported (Nakanishi et al., 1992 and 1994). Among group III mGluRs, which also exhibit the same effect on adenylyl cyclase, stimulatory mGluR6 is totally different from mGluRs4 and 7, which have no apparent coupling. The reason for such discrepancy in coupling modes to ADP-ribosyl cyclase and adenylyl cyclase between mGluRs within the same group is not clear. One possible explanation will be different G-protein selectivity of mGluRs belonging to the same group. Although this is not a direct evidence for mGluRs in group II and IIII, it has been recently shown that mGluR1 and mGluR5 of the same group-I mGluRs, which primarily couple to phospholipase C via the $G_{q/11}$-type G protein, activate the extracellular signal-regulated kinase via distinct signaling pathways, in that mGluR1 utilizes a PTx-sensitive pathway but mGluR5 does not (Thandi et al., 2002).

Taking our findings on coupling to ADP-ribosyl cyclase into consideration, new subclasses in group II and III of mGluRs should be defined (Table 3). Both mGluRs1 and 5 remain in group I, given their identical signal transduction preference. If 'a' is used for mGluRs that activate, 'b' is given to mGluRs that negatively regulate, and 'c' stands for non-coupling receptors, mGluRs1 and 5 belong to group Ia. mGluR3 could be subdivided to group IIa, and mGluR2 into group IIb. The group IIIa subclass includes mGluR6, whereas group IIIc includes mGluRs4 and 7.

Is such sub-classification valid? We believe that new subdivision from functional aspects (i.e., coupling preference) may well accord to the difference in histological localization (Ottersen and Landsend, 1997; Shigemoto et al., 1997; Cartmell and Schoepp, 2000), as listed in Table 3. For instance, mGluRs3 and 2 are located at the same presynaptic regions, but not exactly the same postsynaptic site (Tamaru et al., 2001). In the hippocampal

dentate gyrus, the postsynaptic localization of mGluR3 is rather similar to that of group I mGluRs than mGluR2 (Tamaru et al., 2001). Similarly, while mGluRs4 and 7 are exclusively located presynaptically, mGluR6 shows postsynaptic localization (Nakajima et al., 1993; Nomura et al., 1994; Shigemoto et al., 1997; Neto et al., 2000). Interestingly, closer inspection of Table 3 reveals that coupling to ADP-ribosyl cyclase appears to be restricted to a subset of mGluRs whose postsynaptic existence has been proven. Therefore, such coincidence may support our new classification resulted from more multiple signal transduction pathways than previously appreciated (Nakanishi, 1992 and 1994; Duvoisin et al., 1995; Conn and Pin, 1997; Nakanishi et al., 1998).

The present study is one of the few to describe the possible role of peripheral mGluRs, given that activation of mGluR5 modulates nociception on unmyelinated sensory afferents (Bhave et al., 2001). Judging from our electrophysiological studies on cultured SCG cells, group I mGluRs increase cADP-ribose formation in ganglion neurons. However, glial cells also possess group I mGluRs (Biber et al., 1999), hence a glial contribution to our measurement of ADP-ribosyl cyclase can not be excluded. Preganglionic neurons in the SCG do not release glutamate (Conn and Pin, 1997; Anwyl, 1999), and thus one possibility is that glutamate released from surrounding glial cells may act on mGluR1 or mGluR5 in postganglionic neurons, in vivo. It will be interesting to test if release of acetylcholine from ganglion cells could be modulated by activation of ryanodine receptors by increased cADP-ribose.

mGluR6 has been shown to be located not on the tip of the central element but on its base at the mouth of the invagination, 400-800 nm from the release site in 'ON' bipolar cells (Vardi et al., 2000), and function to transfer on-signaling by depolarizing bipolar cells via opening of cGMP-gated cation channels by light stimulation (de la Villa et al., 1995). These channels could be partially phosphorylated with light by Ca^{2+} (Shiells and Falk, 1999; Nawy, 2000) and CaM-kinase II (Walters et al., 1998; Shiells and Falk, 2000), and should be dephosphorylated by calcineurin in the dark-adapted retina (Shiells and Falk, 2001). If this

explanation is true, a plausible mechanism is that cADP-ribose interacts with calcineurin (Shiells and Falk, 2001), which removes the rectification properties of cGMP-dependent channels (Shiells and Falk, 2001). Alternatively, since Ca^{2+} concentration is increased by caffeine in goldfish or carp retinal bipolar cells (Kobayashi et al., 1995; Wu and Zhu, 1999), cADP-ribose may potentiate this reaction through ryanodine receptors. The physiological relevance of mGluR6-mediated cADP-ribose formation remains to be determined.

The coupling of mGluRs1 and 5 to ADP-ribosyl cyclase via CTx-sensitive G proteins is not surprising, because mGluRs1 and 5 activate phospholipase C (Nakanishi et al., 1992 and 1994; Miyashita and Kubo, 2000; Miura et al., 2002), similarly observed in muscarinic receptor subtypes 1 and 3 (Higashida et al., 1997). However, the involvement of a CTx-sensitive subset of G proteins in mGluR6- and mGluR3-coupling is unexpected, since mGluRs6 and 3 are negatively coupled to adenylyl cyclase via PTx-sensitive G_i/G_o in this and other experiments (Nakanishi et al., 1994). Although the main G protein coupled with mGluR6 is G_o (Vardi, 1998), it has been reported that CTx-sensitive-G_t also weakly but significantly couples to mGluR6 (Weng et al., 1997). However, CTx on this mGluR-mediated activity is perplexing and CTx may not have any direct effects on any G proteins that bridge over mGluRs and ADP-ribosyl cyclase. Further validation is necessary of G protein species-linkage between mGluRs and ADP-ribosyl cyclase. In support of our hypothesis of G protein involvement, recently, cADP-ribose and CD38 were shown to regulate Ca^{2+} responses and chemotaxis of a specific subset of G protein-coupled receptors in human neutrophils (Partida-Sanchez et al., 2001) and endothelin was found to stimulate ADP-ribosyl cyclase via activation of both endothelin A and B receptors (Barone et al., 2002).

In conclusion, we have demonstrated that efficient coupling of mGluRs to ADP-ribosyl cyclase in neuronal tissues occurs in a subtype-specific fashion. The challenge for the future is to define in greater detail the role of cADP-ribose in neurons (Higashida et al., 2001), which may provide greater insight into the mechanisms of mGluR-mediated neuronal function.

Acknowledgements - We thank Masanobu Kano for comments on the manuscript. This work was supported grants from the Ministry of Education, Science, Sports, Culture and Technology of Japan.

References

Abe T., Sugihara H., Nawa H., Shigemoto R., Mizuno N. and Nakanishi S. (1992) Molecular characterization of a novel metabotropic glutamate receptor mGluR5 coupled to inositol phosphate/Ca^{2+} signal transduction. *J. Biol. Chem.* **267**, 13361-13368.

Akita T. and Kuba K. (2000) Functional triads consisting of ryanodine receptors, Ca^{2+} channels, and Ca^{2+}-activated K^+ channels in bullfrog sympathetic neurons. Plastic modulation of action potential. *J. Gen. Physiol.* **116**, 697-720.

Ango F., Prezeau L., Muller T., Tu J. C., Xiao B., Worley P. F., Pin J. P., Bockaert J. and Fagni L. (2001) Agonist-independent activation of metabotropic glutamate receptors by the intracellular protein Homer. *Nature* **411**, 962-5.

Anwyl, R. (1999) Metabotropic glutamate receptors: electrophysiological properties and role in plasticity. *Brain Res. Rev.* **29**, 83-120.

Barone F., Genazzani A. A., Conti A., Churchill G. C., Palombi F., Ziparo E., Sorrentino V., Galione A. and Filippini A. (2002) A pivotal role for cADPR-mediated Ca^{2+} signaling: regulation of endothelin-induced contraction in peritubular smooth muscle cells. *FASEB J.* **16**, 697-705.

Bhave G., Karim F., Carlton S. M. and Gereau R. W. Peripheral group I metabotropic glutamate receptors modulate nociception in mice. (2001) *Nat. Neurosci.* **4**, 417-423.

Biber K., Laurie D. J., Berthele A., Sommer B., Tolle T. R., Gebicke-Harter P. J., van Calker D. and Boddeke H. W. (1999) Expression and signaling of group I metabotropic glutamate receptors in astrocytes and microglia. *J. Neurochem.* **72**, 1671-1680.

Cartmell J. and Schoepp D. D. (2000) Regulation of neurotransmitter release by metabotropic glutamate receptors. *J. Neurochem.* **75**, 889-907.

Chavis P., Fagni L., Lansman J. B. and Bockaert J. (1996) Functional coupling between ryanodine receptors and L-type calcium channels in neurons. *Nature* **382**,719-722.

Chiamulera C., Epping-Jordan M. P., Zocchi A., Marcon C., Cottiny C., Tacconi S., Corsi M., Orzi F. and Conquet F. (2001) Reinforcing and locomotor stimulant effects of cocaine are absent in mGluR5 null mutant mice. *Nat. Neurosci.* **4**, 873-874.

Chuang S. C., Bianchi R. and Wong R. K. (2000) Group I mGluR activation turns on a

voltage-gated inward current in hippocampal pyramidal cells. *J. Neurophysiol.* 83, 2844-2853.

Cooper D. M., Schlegel W., Lin M. C. and Rodbell M. (1979) The fat cell adenylate cyclase system. Characterization and manipulation of its bimodal regulation by GTP. *J. Biol. Chem.* **254**, 8927-8931.

Conn P. J. and Pin J. P. (1997) Pharmacology and functions of metabotropic glutamate receptors. *Annu. Rev. Pharmacol. Toxicol.* **37**, 205-237.

Crawford J. H., Wainwright A., Heavens R., Pollock J., Martin D. J., Scott R. H. and Seabrook G. R. (2000) Mobilisation of intracellular Ca^{2+} by mGluR5 metabotropic glutamate receptor activation in neonatal rat cultured dorsal root ganglia neurones. *Neuropharmacol.* **39**, 621-630.

de la Villa P., Kurahashi T. and Kaneko A. (1995) L-glutamate-induced responses and cGMP-activated channels in three subtypes of retinal bipolar cells dissociated from the cat. *J Neurosci.* **15**, 3571-3582

Duvoisin R. M., Zhang C. & Ramonell K. (1995) A novel metabotropic glutamate receptor expressed in the retina and olfactory bulb. *J. Neurosci.* **15,** 3075-3083.

Empson R. M. and Galione A. (1997) Cyclic ADP-ribose enhances coupling between voltage-gated Ca^{2+} entry and intracellular Ca^{2+} release. *J. Biol. Chem.* **272**, 20967-2070.

Fagni L., Chavis P., Ango F. and Bockaert J. (2000) Complex interactions between mGluRs, intracellular Ca^{2+} stores and ion channels in neurons. *Trends Neurosci.* 23, 80-88.

Graeff R. M., Walseth T. F., Fryxell K., Branton W. D. and Lee H. C. (1994) Enzymatic synthesis and characterizations of cyclic GDP-ribose. A procedure for distinguishing enzymes with ADP-ribosyl cyclase activity. *J. Biol. Chem.* **269**, 30260-30267.

Hannan A. J., Blakemore C., Katsnelson A., Vitalis T., Huber K. M., Bear M., Roder J., Kim D., Shin H. S. and Kind P. C. (2001) PLC-beta1, activated via mGluRs, mediates activity-dependent differentiation in cerebral cortex. *Nat. Neurosci.* **4**, 282-288

Hartveit E., Brandstatter J. H., Enz R. and Wassle H. (1995) Expression of the mRNA of seven metabotropic glutamate receptors (mGluR1 to 7) in the rat retina. An in situ hybridization study on tissue sections and isolated cells. *Eur. J. Neurosci.* **7**, 1472-1483.

Hashii M., Minabe Y. and Higashida H. (2000) cADP-ribose potentiates cytosolic Ca^{2+}

elevation and Ca^{2+} entry via L-type voltage-activated Ca^{2+} channels in NG108-15neuronal cells. *Biochem. J.* **345**, 207-215.

Higashida H., Egorova A., Higashida C., Zhong Z. G., Yokoyama S., Noda M. and Zhang J. S. (1999) Sympathetic potentiation of cyclic ADP-ribose formation in rat cardiac myocytes. *J. Biol. Chem.* **274**, 33348-33354.

Higashida H., Hashii M., Yokoyama S., Hoshi N., Chen X.-L., Egorova A., Noda M. and Zhang J.-S. (2001) Cyclic ADP-ribose as a second messenger revisited from a new aspect of signal transduction from receptors to ADP-ribosyl cyclase. *Pharmacol. Ther.* **90**, 283-296.

Higashida H., Hossain K., Takahagi H. and Noda M. (2002) Measurement of adenylyl cyclase by separating cyclic AMP on silica gel thin-layer chromatography. *Anal. Biochem.* **308,** 106-111.

Higashida H., Yokoyama S., Hashii M., Taketo M., Higashida M., Takayasu T., Ohshima T., Takasawa S., Okamoto H. and Noda M. (1997) Muscarinic receptor-mediated dual regulation of ADP-ribosyl cyclase in NG108-15 neuronal cell membranes. *J. Biol. Chem.* **272**, 31272-31277.

Ikeda S. R., Lovinger D. M., McCool B. A. and Lewis D. L. (1995) Heterologous expression of metabotropic glutamate receptors in adult rat sympathetic neurons: subtype-specific coupling to ion channels. *Neuron* **14**, 1029-1038.

Kobayashi K., Sakaba T. and Tachibana M. (1995) Potentiation of Ca^{2+} transients in the presynaptic terminals of goldfish retinal bipolar cells. *J. Physiol.* **482**, 7-13.

Kuwajima G., Futatsugi A., Niinobe M., Nakanishi S. and Mikoshiba K. (1992) Two types of ryanodine receptors in mouse brain: skeletal muscle type exclusively in Purkinje cells and cardiac muscle type in various neurons. *Neuron* **9**, 1133-1142.

Lee H.-C. (2001) Physiological functions of cyclic ADP-ribose and NAADP as calcium messengers. *Annu. Rev. Pharmacol. Toxicol.* **41**, 317-345.

Liu M. and Kirchgessner A. L. (2000) Agonist- and reflex-evoked internalization of metabotropic glutamate receptor 5 in enteric neurons. *J. Neurosci.* **20**, 3200-3205.

Masu M., Tanabe Y., Tsuchida K., Shigemoto R. and Nakanishi S. (1991) Sequence and expression of a metabotropic glutamate receptor. *Nature* **349**, 760-765.

Miura M., Watanabe M., Offermanns S., Simon M. I. and Kano M. (2002) Group I

metabotropic glutamate receptor signaling via Galpha q/Galpha 11 secures the induction of long-term potentiation in the hippocampal area CA1. *J. Neurosci.* **22**, 8379-9390.

Miyashita T. and Kubo Y. (2000) Extracellular Ca^{2+} sensitivity of mGluR1alpha induces an increase in the basal cAMP level by direct coupling with Gs protein in transfected CHO cells. *Receptors Channels* **7**, 77-91.

Mochida S., Kobayashi H., Matsuda Y., Yuda Y., Muramoto K. and Nonomura Y. (1994) Myosin II is involved in transmitter release at synapses formed between rat sympathetic neurons in culture. *Neuron* **13**, 1131-1142.

Morikawa H., Khodakhah K. and Williams J. T. (2003) Two intracellular pathways mediate metabotropic glutamate receptor-induced Ca^{2+} mobilization in dopamine neurons. *J Neurosci.* **23**, 149-157.

Nomura A., Shigemoto R., Nakamura Y., Okamoto N., Mizuno N. & Nakanishi S. (1994) Developmentally regulated postsynaptic localization of a metabotropic glutamate receptor in rat rod bipolar cells. *Cell* **77**, 361-369.

Nakajima Y., Iwakabe H., Akazawa C., Nawa H., Shigemoto R., Mizuno N. and Nakanishi S. (1993) Molecular characterization of a novel retinal metabotropic glutamate receptor mGluR6 with a high agonist selectivity for L-2-amino-4-phosphonobutyrate. *J. Biol. Chem.* **268**, 11868-11873.

Nakanishi S. (1992) Molecular diversity of glutamate receptors and implications for brain function. *Science* **258**, 597-603.

Nakanishi S. (1994) Metabotropic glutamate receptors: synaptic transmission, modulation, and plasticity. *Neuron* **13**, 1031-1037.

Nakanishi S., Nakajima Y., Masu M., Ueda Y., Nakahara K., Watanabe D., Yamaguchi S., Kawabata S. and Okada M. (1998) Glutamate receptors: brain function and signal transduction. *Brain Res. Rev.* **26**, 230-235.

Nawy S. (2000) Regulation of the on bipolar cell mGluR6 pathway by Ca^{2+}. *J. Neurosci.* **20**, 4471-4479.

Neto F. l., Schadrack J., Berthele A., Zieglgansberger W., Tolle T. R. and Castro-Lopes J. M. (2000) Differential distribution of metabotropic receptor subtype mRNAs in the thalamus of the rat. *Brain Res.* **854**, 93-105.

Okamoto N., Hori S., Akazawa C., Hayashi Y., Shigemoto R., Mizuno N. and Nakanishi S. (1994) Molecular characterization of a new metabotropic glutamate receptor mGluR7 coupled to inhibitory cyclic AMP signal transduction. *J. Biol. Chem.* **269**, 1231-1236.

Ottersen O. P. and Landsend A. S. (1997) Organization of glutamate receptors at the synapse. *Eur. J. Neurosci.* **9**, 2219-2224.

Partida-Sanchez S., Cockayne D. A., Monard S., Jacobson E. L., Oppenheimer N., Garvy B., Kusser K., Goodrich S., Howard M., Harmsen A., Randall T. D. and Lund F. E. (2001) Cyclic ADP-ribose production by CD38 regulates intracellular calcium release, extracellular calcium influx and chemotaxis in neutrophils and is required for bacterial clearance in vivo. *Nat. Med.* **7**, 1209-1216.

Pollock J., Crawford J. H., Wootton J. F., Seabrook G. R. and Scott R. H. (1999) Metabotropic glutamate receptor activation and intracellular cyclic ADP-ribose release Ca^{2+} from the same store in cultured DRG neurones. *Cell Calcium* **26**, 139-148.

Ronde P., Dougherty J. J. and Nichols R. A. (2000) Functional IP3- and ryanodine-sensitive calcium stores in presynaptic varicosities of NG108-15 (rodent neuroblastoma x glioma hybrid) cells. *J. Physiol.* **529**, 307-319

Servitja J. M., Masgrau R., Sarri E. and Picatoste F. (1999) Group I metabotropic glutamate receptors mediate phospholipase D stimulation in rat cultured astrocytes. *J. Neurochem.* **72**, 1441-1447.

Shiells R. A. and Falk G. (1999) A rise in intracellular Ca^{2+} underlies light adaptation in dogfish retinal 'on' bipolar cells. *J. Physiol.* **514**, 343-350.

Shiells R. A. and Falk G. (2000) Activation of Ca^{2+}--calmodulin kinase II induces desensitization by background light in dogfish retinal 'on' bipolar cells. *J. Physiol.* **528**, 327-338.

Shiells R. A. and Falk G. (2001) Rectification of cGMP-activated channels induced by phosphorylation in dogfish retinal 'on' bipolar cells. *J. Physiol.* 535, 697-702.

Shigemoto R., Kinoshita A., Wada E., Nomura S., Ohishi H., Takada M., Flor P. J., Neki A., Abe T., Nakanishi S. and Mizuno N. (1997) Differential presynaptic localization of metabotropic glutamate receptor subtypes in the rat hippocampus. *J. Neurosci.* **17**, 7503-7522.

Sugihara H., Inoue T., Nakanishi S. and Fukuda Y. (1997) A late ON response remains in

visual response of the mGluR6-deficient mouse. *Neurosci. Lett.* 233, 137-140.

Takahashi K., Kukimoto I., Tokita K., Inageda K., Inoue S., Kontani. K, Hoshino S., Nishina H., Kanaho Y. and Katada T. (1995) Accumulation of cyclic ADP-ribose measured by a specific radioimmunoassay in differentiated human leukemic HL-60 cells with all-trans-retinoic acid. *FEBS Lett.* 371, 204-208.

Tamaru Y., Nomura S., Mizuno N. and Shigemoto R. (2001) Distribution of metabotropic glutamate receptor mGluR3 in the mouse CNS: differential location relative to pre- and postsynaptic sites. *Neurosci.* **106**, 481-503.

Tanabe Y., Masu M., Ishii T., Shigemoto R. and Nakanishi S. (1992) A family of metabotropic glutamate receptors. *Neuron* **8**, 169-179.

Thandi S., Blank J. L. and Challiss R. A. (2002) Group-I metabotropic glutamate receptors, mGlu1a and mGlu5a, couple to extracellular signal-regulated kinase (ERK) activation via distinct, but overlapping, signalling pathways *J. Neurochem.* **8**, 1139-1154.

Vardi N. (1998) Alpha subunit of Go localizes in the dendritic tips of ON bipolar cells. *J. Comp. Neurol.* **395**, 43-52.

Walters R. J., Kramer R. H. and Nawy S. (1998) Regulation of cGMP-dependent current in On bipolar cells by calcium/calmodulin-dependent kinase. *Vis. Neurosci.* **15**, 257-621.

Weng K., Lu C., Daggett L. P., Kuhn R., Flor P. J., Johnson E. C. & Robinson P. R. (1997) Functional coupling of a human retinal metabotropic glutamate receptor (hmGluR6) to bovine rod transducin and rat Go in an in vitro reconstitution system. *J. Biol. Chem.* **272**, 33100-33104.

Wu, D. and Zhu, P. H. (1999) Caffeine-sensitive Ca^{2+} stores in carp retinal bipolar cells. *Neuroreport* **10**, 3897-3901.

Table 1

Effects of glutamate and group-specific agonists on cGDP-ribose formation in rat retina and SCG

Group-specific agonist	ADP-ribosyl cyclase activity (% of pre-addition level)		
	Initial application of agonist	Subsequent application of glutamate	Δ Increase (%)
Retina			
None	-	167.5 ± 16.9 (9)*	-
I (DHPG)	102.3 ± 2.3 (4)	173.0 ± 6.6 (4)**	70.7***
II (DCG-IV)	100.3 ± 0.4 (3)	158.5 ± 10.8 (3)*	58.2***
III (L-AP4)	172.3 ± 8.6 (5) **	194.0 ± 8.2 (5)**	21.7
SCG			
None	-	164.8 ± 5.2 (5)**	-
I (DHPG)	173.3 ± 4.3 (4)**	178.8 ± 5.7 (4)**	5.5
II (DCG-IV)	111.3 ± 6.6 (3)	171.0 ± 4.7 (3)**	59.7***
III (L-AP4)	107.3 ± 1.3 (3)	174.7 ± 9.4 (3)**	67.4***

Cell membranes were incubated with 60 μM β-NAD^+, and the fluorescence of the resulting cGDP-ribose continuously monitored. Activity after application of 10 nM DHPG, DCG-IV, and L-AP4 was measured and calculated as percentage of the pre-application level, respectively. Subsequently, 10 nM glutamate was added. It is noted that only little increase was obtained by glutamate in the presence of L-AP4 or DHPG in retina and SCG. * and **, significantly different from control values (without agonists) at $p < 0.05$ and 0.001. ***, significantly different between values of initial application with agonists and subsequent application with glutamate at $p < 0.01$.

Table 2

Effect of glutamate on cGDP-ribose formation in the presence of each group-specific antagonist in rat retina and SCG.

Group-specific antagonist	Glutamate-induced activation (%)	
	Retina	SCG
I (AIDA)	159.5 ± 20.2 (4)*	103.0 ± 4.3 (4)
II (EGLU)	147.0 ± 5.0 (3)**	185.7 ± 1.5 (3)**
III (CPPG)	102.3 ± 1.5 (3)	185.3 ± 8.6 (3)**

Glutamate (10 nM) was applied in the presence of 10 μM antagonists. * and **, significantly different from the control value at $p < 0.05$ and $p < 0.001$.

Table 3

Subclassification of mGluRs according to coupling preference and localization in synaptic regions.

Group	Subtype	Coupling to			Synaptic localization*	
		NC**	AC**	PLC**	Presynaptic	Postsynaptic
I a	mGluR1	↑	↑	↑	-	Peri, Extra
I a	mGluR5	↑	↑	↑	-	Peri, Extra
II a	mGluR3	↑	↓		Extra	PSD, Peri, Extra
II b	mGluR2	↓	↓		Extra	Extra
III a	mGluR6	↑	↓		-	BCE
III c	mGluR4	→	↓		Active zone	-
III c	mGluR7	→	↓		Active zone	-

*Based upon observations described in the text. Peri, perisynaptic site; Extra, extrasynaptic site; PSD, postsynaptic density; BCE, base of central element; -, not detected.

**NC, ADP-ribosyl cyclase; AC, adenylyl cyclase; PLC, phospholipase C.

↑, activation; ↓, inhibition; →, no effect.

Figure legends

Fig. 1. Activation of ADP-ribosyl cyclase by glutamate in rat retina and SCG. ADP-ribosyl cyclase was measured from the initial velocity during 2 min with membranes prepared from rat retina (A) and SCG (B). Values were calculated by conversion of [^{3}H]cADPR from [^{3}H]NAD$^+$ in the presence or absence of 10 μM glutamate in 4 experiments. Values indicate mean ± S.E.M. * indicates significantly different from the control at $p < 0.01$.

Fig. 2. Effect of glutamate on cGDP-ribose-producing activity in retina and SCG. Plot shows relationship between concentrations of glutamate and cGDP-ribose formation in retina (square) and SCG (circle), olfactory bulb (downward triangle), cerebral cortex (right-ward triangle), hippocampus (upward triangle), cerebellum (diamond). Data represent mean ± S.E.M. for 3-9 measurements. Values at 1 nM or higher concentrations of glutamate are significantly different ($p < 0.02$) from control activity (100% without agonists) in both retina and SCG. Inset, cell membranes isolated from retina (upper, 55.4 μg) and SCG (lower, 35.7 μg) of 5-week-old rats were incubated with 60 μM β-NGD$^+$, and the fluorescence of the resulting cGDP-ribose continuously monitored. At the time indicated by arrow, 10 μM glutamate at the final concentration was added.

Fig. 3. Effects of various concentrations of group-specific agonists on cGDP-ribose-producing activity in rat retina (A) and SCG (B). Relationship between concentrations of L-AP4 (diamond, III), DCG-IV (circle, II), or DHPG (triangle, I) and cGDP-ribose formation. The fluorescence of the resulting cGDP-ribose was continuously monitored, and the velocity of cGDP-ribose formation calculated as shown in Fig. 2. Changes in fluorescence induced by application of indicated concentrations of the 3 agonists and glutamate (square, G), as in Fig. 2, were

plotted. Data represent mean ± S.E.M. for 3-9 measurements. Values at 1 nM of L-AP4 in A and DHPG in B are significantly different ($p < 0.02$) from the control activity (100% without agonists) and all other values of L-AP4 in A and DHPG in B are at $p < 0.001$.

Fig. 4. Effect of glutamate on ADP-ribosyl cyclase activity in retina and SCG of wild-type and mGluR6 deficient mice. 1 μM glutamate induced activation of ADP-ribosyl cyclase activity in membranes of retina (A) and SCG (B) of wild-type (+/+) or mGluR6-knockout mice (-/-). Data represent 6-8 measurements from three 12-month-old mice of each type. Bars= S.E.M. *, $p < 0.001$.

Fig. 5. Chart-recordings of membrane potential changes in cultured rat SCG neurons induced by glutamate and a group I agonist. (A, B) Three hundred μM glutamate was added to the bath (arrows), in the absence (A) and the presence of 100 μM AIDA (B). (C) DHPG was added to the bath producing 1.5 μM. The resting membrane potential of the SCG neurons was –51 mV (A), -53 mV (B) and –52 mV (C), respectively. (Inset) Peak amplitude of slow depolarizations was measured and averaged from five experiments with 300 μM glutamate (A), five experiments with glutamate in the presence of 100 μM AIDA (B), and eight experiments with 1.5 μM (S)-5,5-DHPG (C). Values represent the mean ± SEM was plotted.

Fig. 6. Effect of GTP on cGDP-ribose-producing activities in retina and SCG. Changes in fluorescence induced by application of indicated concentrations of GTP were plotted in retina (A) and SCG (B) of 5-week-old rats. Each data point represents the mean ± S.E.M of 3-11 determinations. Values at 0.1 nM of GTP in A and B are significantly different at $p < 0.05$ from the control activity. Values for 10 and 100 μM are at $p < 0.01$, and all other values at $p < 0.001$. (C) Changes in

fluorescence induced by application of 10 nM glutamate in the presence of indicated concentrations of GTP were plotted in retina (square) and SCG (circle). Each data point represents the mean ± S.E.M. of 6 or 4 determinations in retina and SCG, respectively. All values are significantly different at $p < 0.01$ from the control activity in both retina and SCG.

Fig. 7. Effects of pretreatment of rats or NG108-15 cells with CTx or PTx on glutamate-induced changes in ADP-ribosyl cyclase activity. Rats (A) or cells stably over-expressing mGluRs1, 3 and 6 (B) or mGluR2 (C) were intraperitoneally injected or incubated with CTx or PTx (100 ng/body weight or /ml) 8-16 h before being tested. Membranes of retina and SCG (A) or NG108-15 cells (B and C) treated (+) or untreated (-) were incubated and ADP-ribosyl cyclase activity determined before and after 1 μM glutamate application. Data represent the mean (± S.E.M.) of 3-6 determinations. * and #, significantly different from non-treated control values at $p < 0.01$ or $p < 0.05$, respectively.

Fig. 8. Glutamate-induced activation or inhibition of ADP-ribosyl cyclase activity in various NG108-15 cells over-expressing mGluRs. ADP-ribosyl cyclase activity was measured with membranes prepared from NG108-15 cells, mock-transfected cells, or NG108-15 cells transiently transfected to express mGluRs1-7. The level of activity was compared in the presence or absence of 10 nM glutamate in the reaction mixture. Data represent means of 3-10 determinations. Bars represent S.E.M. * and #, significantly different from non-transfected (101.3%) and mock-transfected (108.1%) values, at $p < 0.001$ or 0.005, respectively.

Figure 1

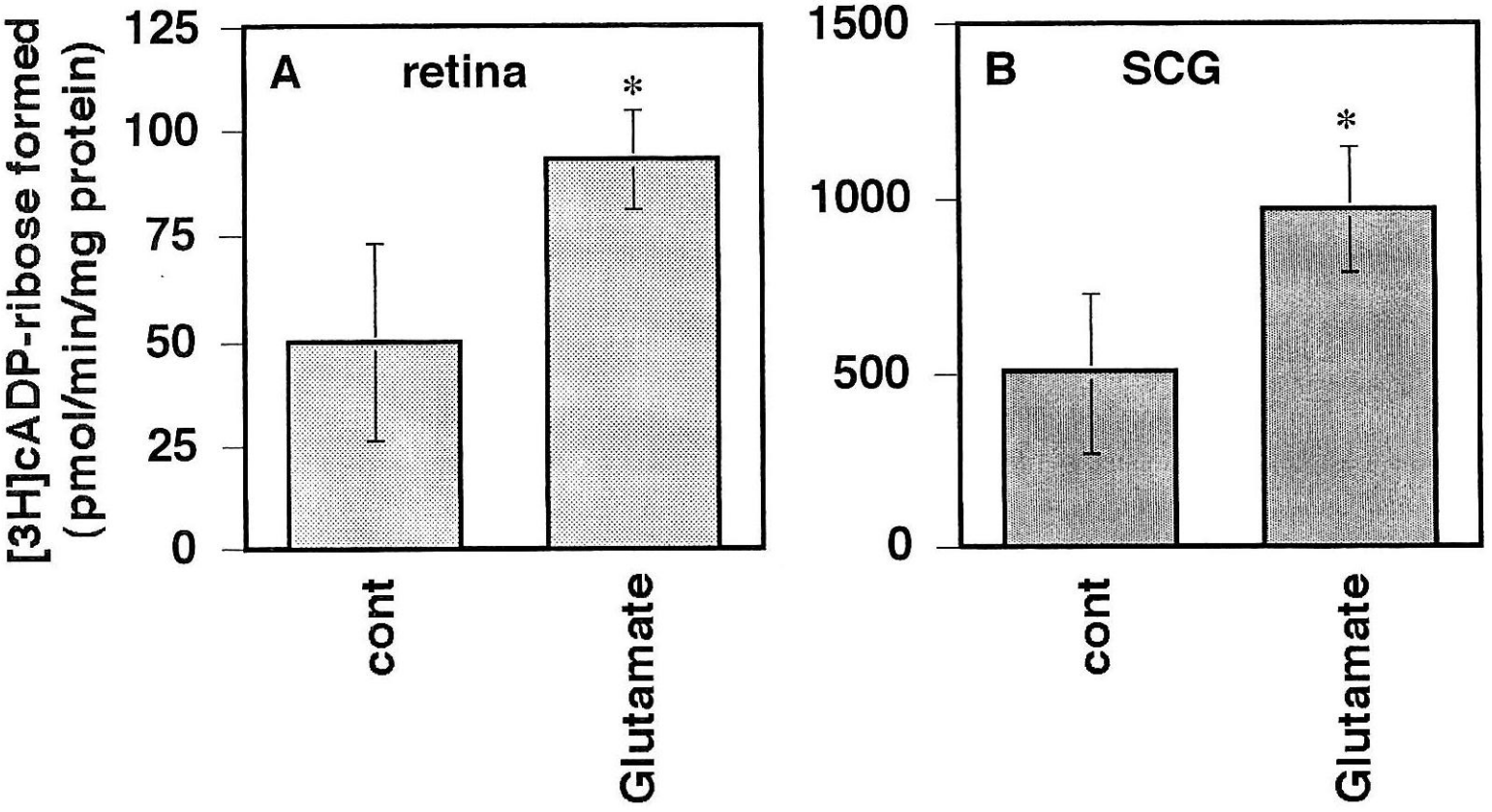
[3H]cADP-ribose formed
(pmol/min/mg protein)
125
100
75
50
25
0
A
retina
*
cont
Glutamate
1500
1000
500
0
B
SCG
*
cont
Glutamate

Figure 2

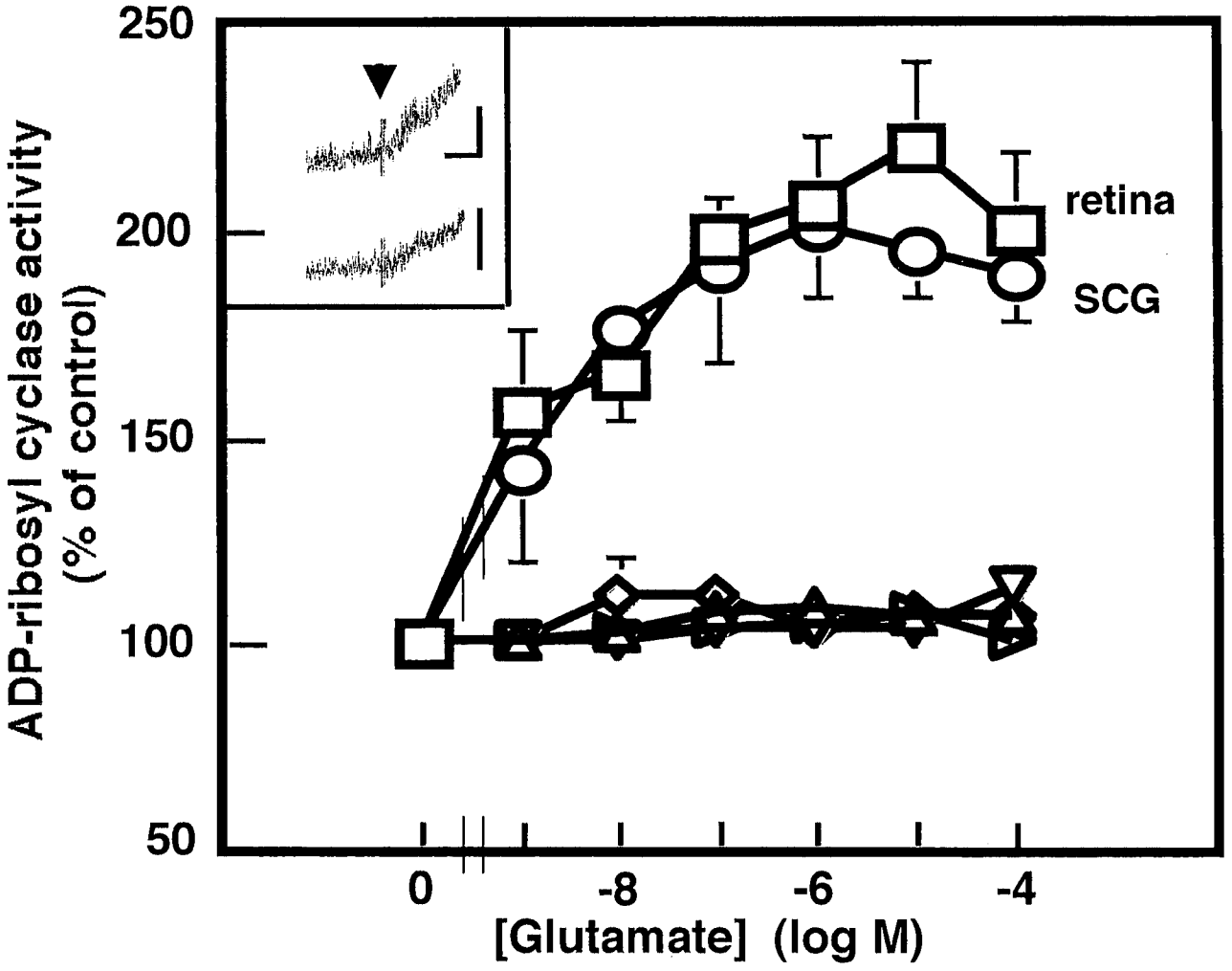
250
200
150
100
50
ADP-ribosyl cyclase activity
(% of control)
retina
SCG
0
-8
-6
-4
[Glutamate] (log M)

Figure 3

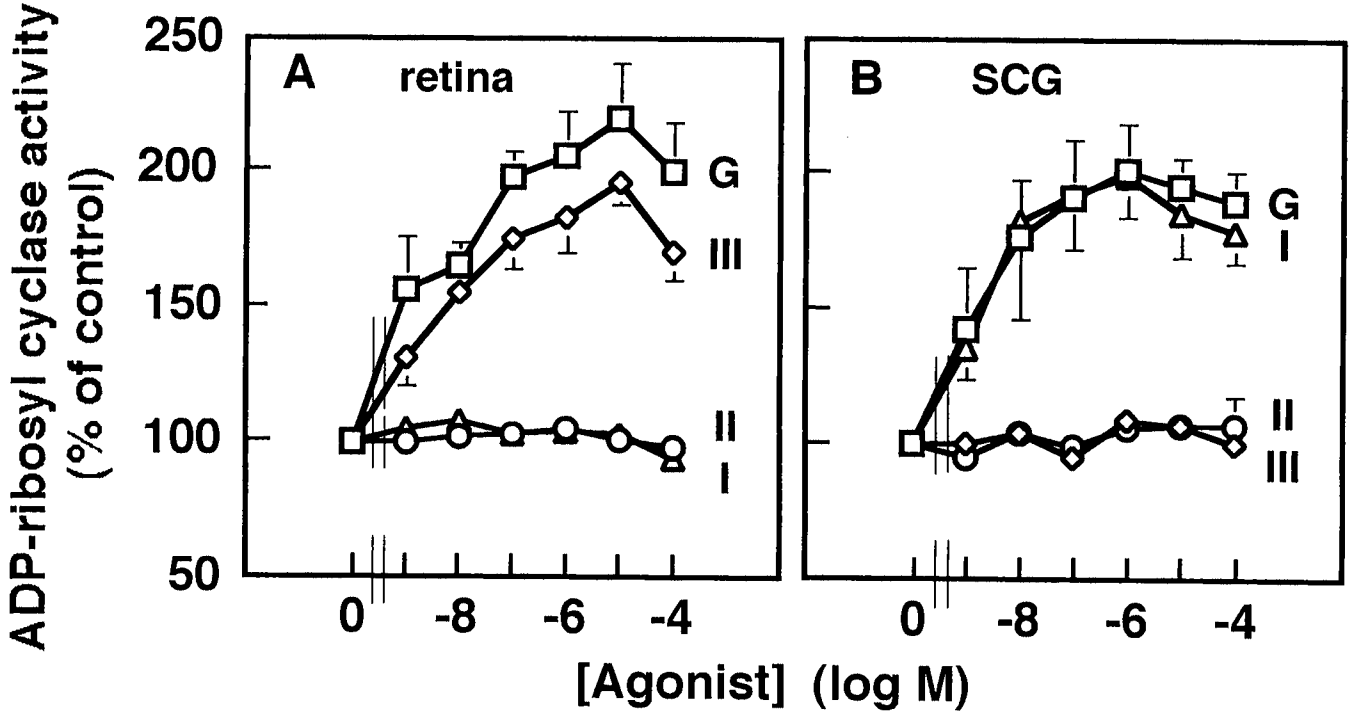
ADP-ribosyl cyclase activity
(% of control)
250
200
150
100
50
A
retina
B
SCG
G
III
II
I
0
-8
-6
-4
[Agonist] (log M)

Figure 4

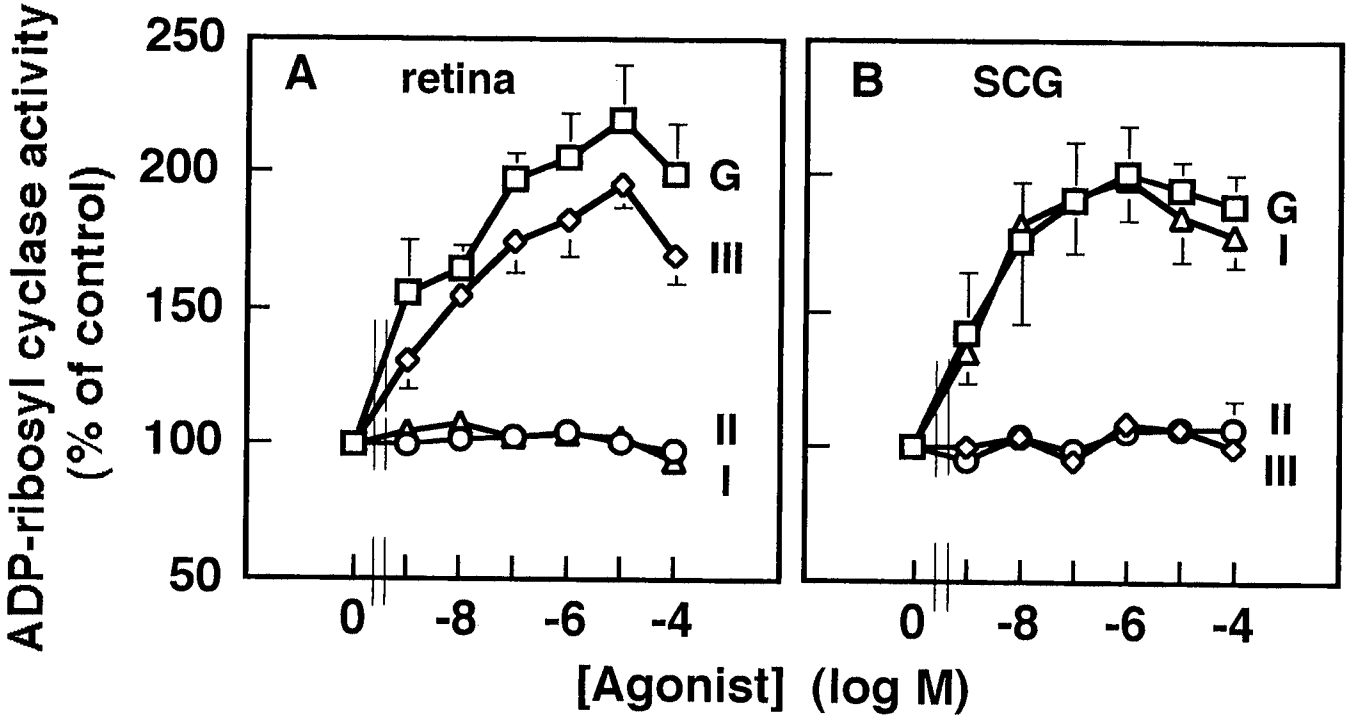
ADP-ribosyl cyclase activity
(% of control)
250
200
150
100
50
A
retina
G
III
II
I
0
-8
-6
-4
B
SCG
G
I
II
III
0
-8
-6
-4
[Agonist] (log M)

Figure 5

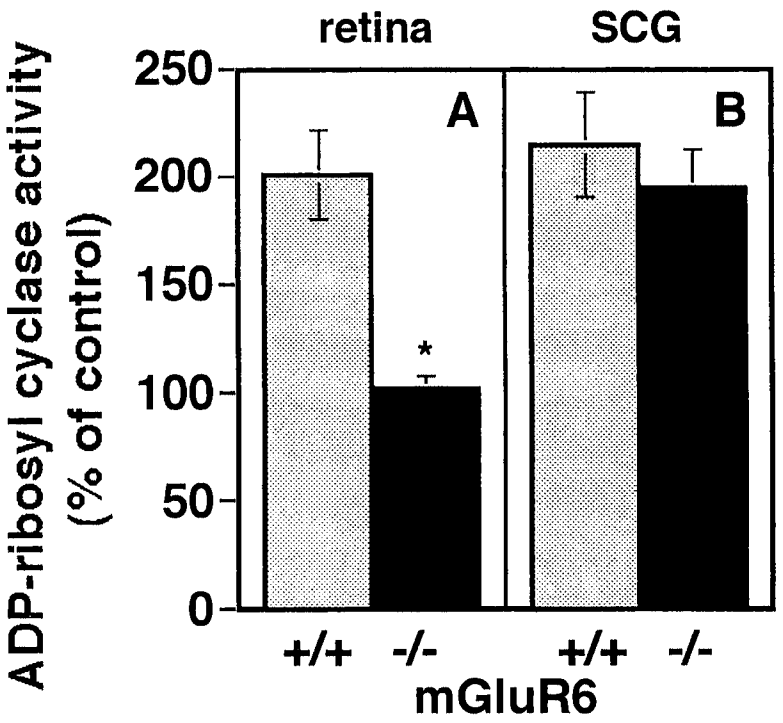
retina
SCG
A
B
250
200
150
100
50
0
*
ADP-ribosyl cyclase activity
(% of control)
+/+
-/-
+/+
-/-
mGluR6

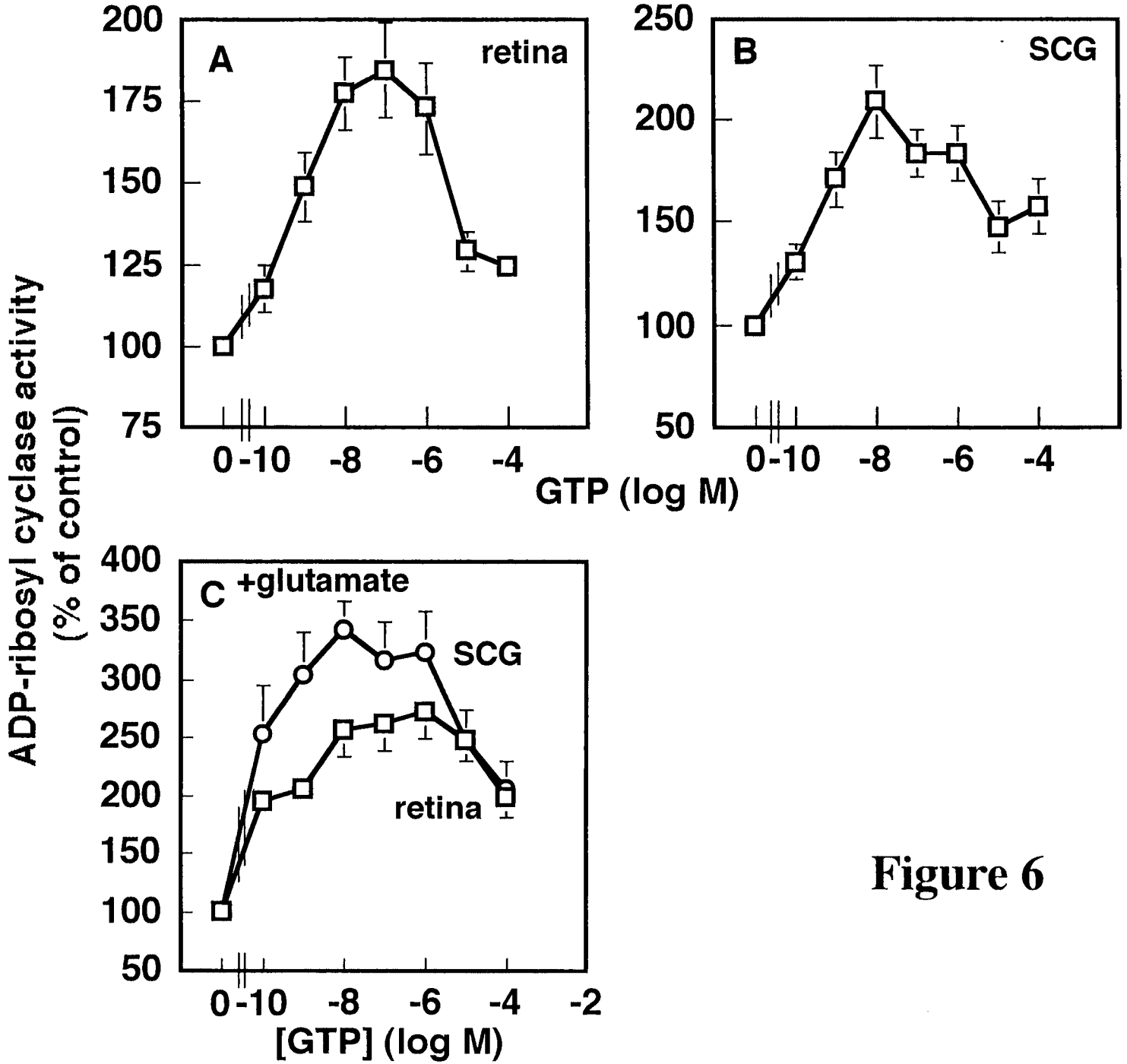
A
retina
B
SCG
C +glutamate
SCG
retina
ADP-ribosyl cyclase activity
(% of control)
GTP (log M)
[GTP] (log M)
200
175
150
125
100
75
250
200
150
100
50
400
350
300
250
200
150
100
50
0
-10
-8
-6
-4
-2

Figure 6

Figure 7

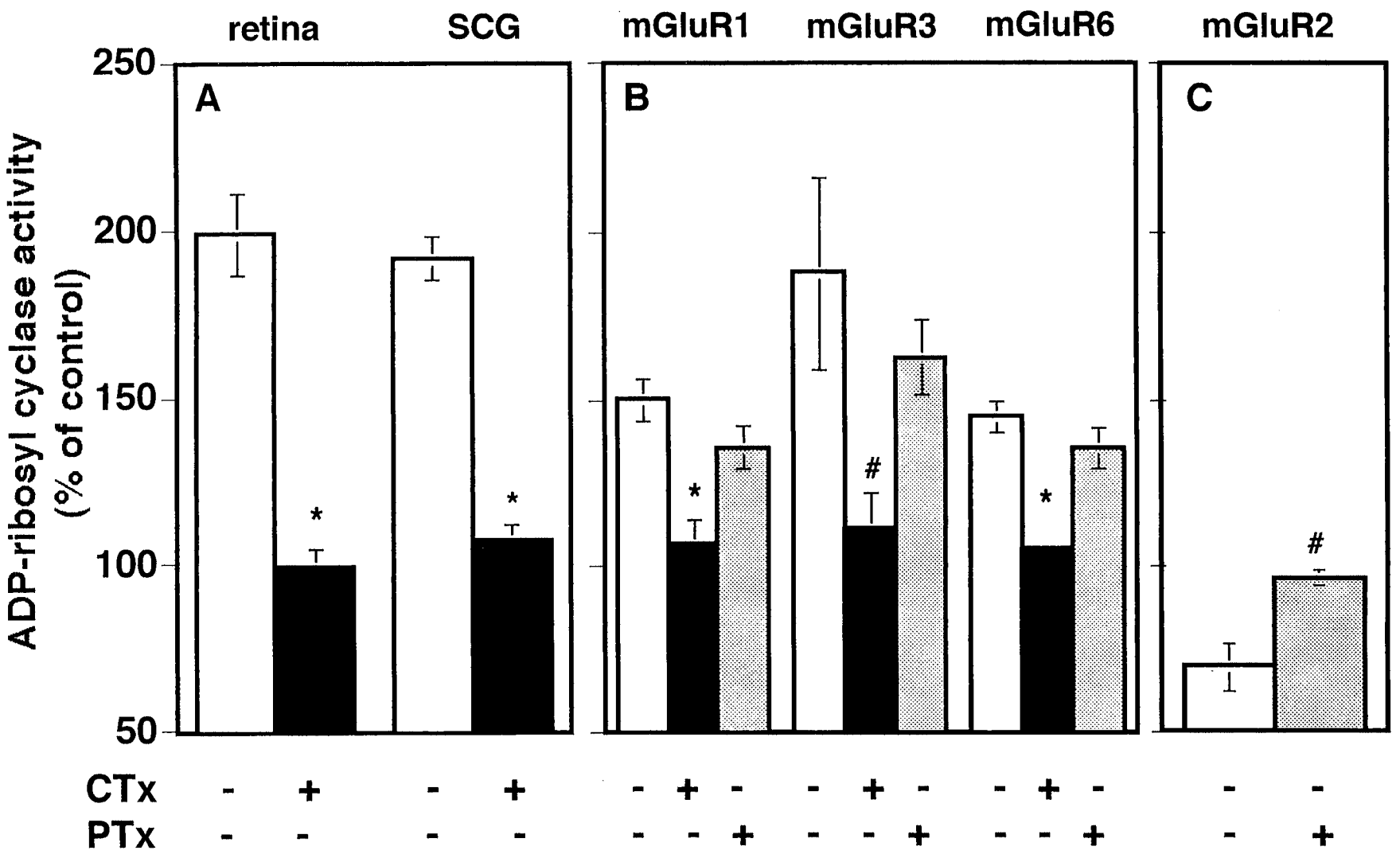
retina
SCG
mGluR1
mGluR3
mGluR6
mGluR2
A
B
C
ADP-ribosyl cyclase activity
(% of control)
250
200
150
100
50
*
*
*
*
#
#
CTx - + - + - + - - + - - + - - - -
PTx - - - - - - + - - + - - + - +

Figure 8

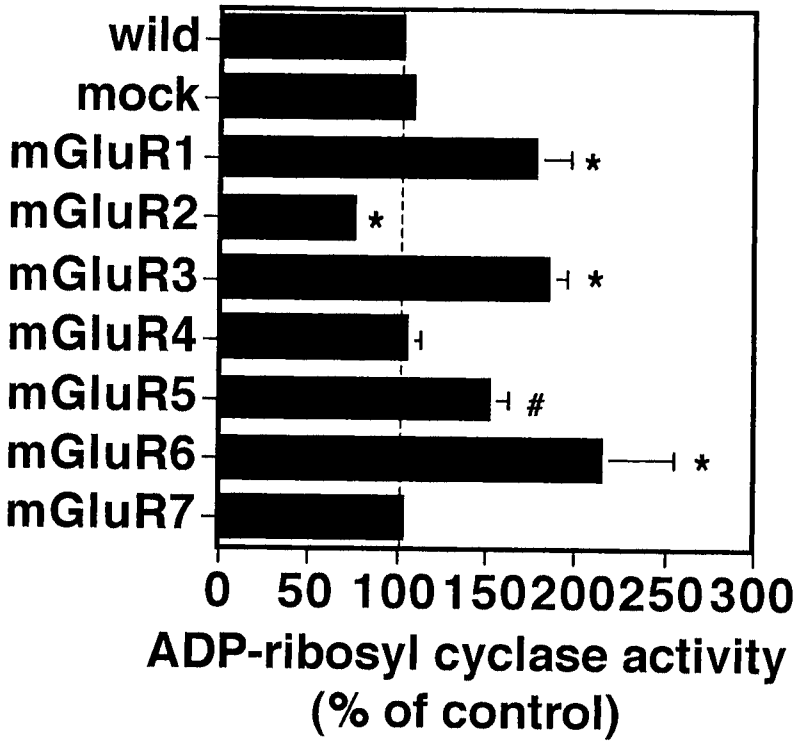
wild
mock
mGluR1
mGluR2
mGluR3
mGluR4
mGluR5
mGluR6
mGluR7
*
*
*
#
*
0 50 100 150 200 250 300
ADP-ribosyl cyclase activity
(% of control)

Part II

Genetic Manipulations of CD38/ADP-Ribosyl Cyclase Alter Acetylcholine-Induced M-Current Inhibition in Superior Cervical Ganglion Neurons and Neuroblastoma Cells

Key Words: cyclic ADP-ribose, CD38, M-current, ADP-ribosyl cyclase, potassium current, muscarinic receptor.

Abstract

The role of ADP-ribosyl cyclase/CD38 in muscarinic acetylcholine receptor (mAChR)-activated inhibition of voltage-gated M potassium currents was examined in normal rats and mice, CD38 knockout mice, and CD38-transformed NG108-15 cells. Application of ACh or other mAChR agonists increased ADP-ribosyl cyclase activity by 200-350% in crude membrane fractions from rat superior cervical ganglia (SCG). This increase was inhibited by atropine or by an M1-mAChR antagonist, pirenzepine, and was mimicked by GTP. ADP-ribosyl cyclase activity in membrane fraction from SCG of CD38 knockout ($CD38^{-/-}$) mice was negligible. M current inhibition by ACh in cultured SCG neurons from $CD38^{-/-}$ mice was greatly reduced compared with that in neurons from wild-type ($CD38^{+/+}$) mice. Cloned M1-mAChR-transformed NG108-15 neuroblastoma x glioma hybrid cells over-expressing human CD38 which has been modified to only display ADP-ribosyl cyclase activity were developed. In these cells, ACh-induced inhibition of the fast (KCNQ) component of the M-like current ($I_{K(M,ng)}$) was significantly greater than in control cells. Inhibition of the slow (ERG) component of $I_{K(M,ng)}$ was largely unchanged, and the voltage dependent gating parameters of $I_{K(M,ng)}$ were not significantly different between the cell types tested. Thus, the extent of ACh-induced KCNQ/M-current inhibition positively correlated with ADP-ribosyl cyclase activity and/or CD38 expression level. These results suggest that the cADPR/ADP-ribosyl cyclase signalling system plays a role in KCNQ/M current inhibition following mAChR stimulation.

Introduction

Cyclic ADP-ribose (cADPR) is an endogenous modulator of ryanodine receptor Ca^{2+} releasing channels (Lee, 1997, 2001). In neurons, cADPR facilitates the release of Ca^{2+} from ryanodine-sensitive stores when Ca^{2+} entry is evoked through voltage-dependent Ca^{2+} channels (an 'orthograde' signal: Hua et al., 1994; Empson and Galione, 1997). There is also a 'retrograde' signal, since Ca^{2+} influx through N- or L-type Ca^{2+} channels can be modulated by activating type 2 ryanodine receptors (Davies et al., 1996; Chavis et al., 1996). Hashii et al. (2000) demonstrated that cADPR is involved in this bi-directional coupling between ryanodine receptors and neuronal Ca^{2+} channels in NG108-15 cells (Higashida et al., 2001a, b).

The key enzyme responsible for synthesis of cADPR is ADP-ribosyl cyclase (Kim et al., 1993; Lee, 1997, 2001; Higashida et al., 1997, 2001a, 2001b). ADP-ribosyl cyclase is a multi-functional ectoenzyme, catalysing both the synthesis of cADPR from β-NAD^+ and the hydrolysis of cADPR to ADP-ribose (Summerhill et al., 1993; Takasawa et al., 1993b). This enzyme is homologous to the mammalian T and/or B cell surface marker CD38 (Jackson and Bell, 1990; States et al., 1992; Harada et al., 1993; Koguma et al., 1994; Prasad et al., 1996). CD38 null mutant mice ($CD38^{-/-}$) show impaired ADP-ribosyl cyclase activity; In such mice, blood sugar level is significantly higher and ryanodine-sensitive Ca^{2+} signalling is attenuated in pancreas, compared to wild type animals (Kato et al., 1999; Fukushi et al., 2001). It has been shown that cysteine residues at 119th and 201st positions found in the human (h)CD38 sequence are involved in the cADPR hydrolase reaction (Takasawa et al., 1993b; Tohgo et al., 1994). Replacing these cysteines (C119K/C201E) converts hCD38 to a monofunctional enzyme with only cADPR synthesizing activity (Tohgo et al., 1994).

In previous experiments (Higashida et al., 1995; Higashida et al., 1996; Bowden et al., 1999; Higashida et al., 2000a), we have obtained information to suggest that cADPR may modulate the M-like K^+ current ($I_{K(M,ng)}$) in NG108-15 mouse neuroblastoma x rat glioma hydrid cells, and may play a part in the inhibition of this current by muscarinic acetylcholine-receptor (mAChR) stimulation. Thus, stimulation of those muscarinic receptors that couple to $I_{K(M,ng)}$ (M1 and M3 receptors: Fukuda et al., 1988; Robbins et al., 1991 and 1993), but not M2 or M4 receptors, stimulated ADP-ribosyl cyclase activity in membrane fractions from these cells (Higashida et al., 1997); elevation of the precursor to cADPR (NAD^+) reduced M1-mAChR-induced $I_{K(M,ng)}$ inhibition (Higashida et al., 1995); intracellular application of cADPR via the patch-pipette accelerated 'run-down' of $I_{K(M,ng)}$ (Higashida et al., 1995); and intracellular application of the cADPR antagonists, 8-amino-cADPR and 8-bromo-cADPR reduced M1-mAChR-induced inhibition of $I_{K(M,ng)}$ (Bowden et al., 1999).

The M-like current in NG108-15 cells is a composite current, carried in part by currents

through KCNQ2/3 channels (the molecular correlates of the M channel in sympathetic neurons: Wang et al., 1998), and in part by currents through mERG channels (Meves et al., 1999; Selyanko et al., 1999). Although both components appear to be affected by cADPR, and although both are inhibited by M1-mAChR stimulation in a manner sensitive to cADPR antagonists (Higashida et al., 2000a), the presence of the two components adds complexity to the interpretation of the above experiments.

Accordingly, in the present experiments, we have sought further information regarding the role of cADPR in M current regulation. First, we have tested whether M1-mAChR stimulation increases ADP-ribosyl cyclase activity in membrane fractions from rat superior cervical sympathetic ganglia (SCGs), the neurons of which only appear to express KCNQ currents, not ERG currents (Selyanko et al., 2002). Second, we have compared M1-mAChR-induced inhibition in sympathetic neurons from wild-type ($CD38^{+/+}$) and $CD38^{-/-}$ null mutant mice. Third, we have tested the effect of over-expressing the cADPR hydrolase-deficient CD38 mutant on M1-mAChR-induced inhibition of $I_{K(M,ng)}$ in NG108-15 cells.

Methods and Materials

Materials

β-[2,8-adenine-^{3}H]NAD^+ (30.5 Ci $mmol^{-1}$) was purchased from New England Nuclear (Boston, MA, U.S.A.). cADPR was obtained from either Yamasa Shoyu (Choshi, Japan) or Sigma (St Louis, MO, U.S.A.). Oxidized-nicotinamide guanine dinucleotide (β-NGD^+) was obtained from Sigma. Silica Gel 60 F254 plastic TLC sheets were obtained from Merck (Darmstadt, Germany).

Mice

Mice lacking CD38 were generated by homologous recombination. The generation and genotyping of the mice have been described in detail previously (Kato et al., 1999; Fukushi et al., 2001). The mice used for each experiment were derived from ICR background and were from the same litter or the same family. Sympathetic neurons were isolated from SCG of humanely killed 14- to 21-d-old mice and cultured using standard procedures as described previously (Selyanko et al., 2002).

Cell culture of NG108-15 ells and CD38 transfection

Neuroblastoma x glioma NG108-15cells over-expressing the M1 muscarinic receptor (NGM1; Fukuda et al., 1988 and 1989) were cultured as described previously (Higashida et al., 1986). Briefly cells were maintained at 37 °C and 10% CO_2 in Dulbecco's modified Eagle's

medium supplemented with 5% foetal calf serum 100 μM hypoxanthine, 0.1 μM aminopterin and 16 μM thymidine. The expression plasmids pZHCD38 and pZHCMCD38 were constructed as follows. The 0.55 Kb *Hind*III (vector)/*Pst*I (606) fragment and 0.36-kb *Pst*I (606)/*Bgl*II (969) fragment from pSV2-HCD38 (Takasawa et al., 1993b) were ligated with 3.0-kb *BamH*I/*Hind*III fragment from pBSIIKS(+) to yield pBSHCD38. Restriction endonuclease sites are identified by numbers in parentheses indicating the 5'-terminal nucleotide generated by cleavage. The 0.91-kb *Hind*III (vector)/*Spe*I (vector) fragment containing the entire protein-coding sequence from pBSHCD38 was ligated with 3.4-kb *Spe*I/*Hind*III fragment from the expression vector pZeoSV to yield pZHCD38 and pZHCMCD38. The plasmids were multiplied in E. coli and purified with a plasmid DNA purification kit (Qiagen, Germany).

NGM1, m1 muscarinic receptor transformed NG108-15 cells were plated in six 35-mm dishes at a density 7.5 x 10^4 cells per dish. After 24 hours the cells were transfected with 10 μg of pZHCD38 or pZHCMCD38 mixed with 25 μg lipofectamine (Bethesda Research laboratories Life Technologies Inc., USA). One day after transfection, the cells were harvested and plated in twelve 60-mm dishes. One week later the cells were selected with 200, 250 and 500 μg ml^{-1} Zeocin. Independent colonies were obtained from cells treated with 200 μg ml^{-1} Zeocin after 4 weeks.

Membrane preparation

Both sexes of Wistar rats (1 to 4 weeks old) and wild-type or $CD38^{-/-}$ mice (3-4 weeks old) were anaesthetized using diethylether and decapitated. SCGs were isolated and minced. NG108-15 cells frozen at –80 °C were thawed. Nervous tissues or cells were then suspended in a hypotonic solution (10 mM Tris-HCl, pH 7.3, with 5 mM $MgCl_2$) at 4°C for 30 min. The cell suspensions were homogenized and the resultant homogenate centrifuged at 4°C for 5 min at 1000 x g to remove unbroken cells and nuclei. Crude membrane fractions were prepared by centrifugation (twice) of homogenates at 105,000 x g for 15 min. The supernatant was removed and the pellet was washed twice, the final pellet was dispersed in 10 mM Tris-HCl solution, pH 6.9, and used immediately for enzymatic reactions. Protein was measured by the BioRad assay dye reagent.

ADP-ribosyl cyclase and cADP-ribose hydrolase assay

Cell membranes (1.2-6 μg), prepared as above, where placed in 20 μl of reaction mixture containing Tris-HCl (50 mM, pH 6.6), 100 mM KCl, 5 mM $MgCl_2$, 0.1 mM EDTA, 2 μMNAD$^+$, [^{3}H] β-NAD$^+$ (0.11 μM, 0.06 μCi) slightly modified to what was reported previously (Higashida et al., 1997). Reaction mixtures were incubated for 0.5 to 16 min at 37

°C and stopped by the addition of 2 µl trichloroacetic acid (10-48%). Aliquots were centrifuged (14,000 x g, 2.5 min) and 2 µl of the supernatant was spotted on silica gel plastic thin layer chromatography (TLC) sheets (20 x 10 cm). The layer was developed in the ascending direction for 40-60 min at 24 °C in a mixture consisting of 30% water, 70% ethanol and 0.2 M ammonium bicarbonate (Higashida et al., 1999). The positions of authentic cADPR, ADPR and β-NAD^+ after UV detection were confirmed in each run. Corresponding positions on the experimental runs were cut out of the gel (about 1 cm by 0.7 cm) and the radioactivity counted in a liquid scintillation counter. Autoradiography of TLC with [^{3}H]β-NAD^+ was obtained after exposure (24 - 36 hours) on a [^{3}H] imaging plate (Fuji BAS1000, Tokyo, Japan). cADPR hydrolase activities were also assayed in 20-μl reaction mixtures contained 2 μM [^{3}H]cADPR (0.015 μCi), according to a previously described formula (Higashida et al., 1997).

Fluorometrical measurement of ADP-ribosyl cyclase

ADP-ribosyl cyclase activity was determined fluorometrically using a technique based on the measurement of the conversion of β-NGD^+ into the fluorescent product cGDPR, as described previously (Graeff et al., 1994; Higashida et al., 1999). Briefly, 2.4 ml of reaction mixtures containing 60 µM β-NGD^+, 50 mM Tris-HCl, pH 6.9, 100 mM KCl, 10 µM $CaCl_2$ and membranes (1.5-50 µg of protein) were maintained at 37°C with constant stirring. The samples were then excited at 300 nm and fluorescence emission was continuously monitored at 410 nm in a Shimadzu RF-5300PC spectrofluorophotometer (Kyoto, Japan). Enzyme activity was determined as the slope of curves computed from data points obtained every 60 ms, and confirmed by curve fitting of smoothing-processed data.

Electrophysiology

The whole cell variant of the patch-clamp technique was employed to record membrane currents from SCG neurons after 2 days in culture or from NG108-15 cells at 4 to 14 days after differentiation, as described in Robbins et al. (1993). Cells were superfused, at 5-10 ml/min, with Hepes-buffered MEM or DMEM or a solution containing 120 mM NaCl, 3 mM KCl, 11 mM glucose, 22.6 mM $NaHCO_3$, 1.2 mM $MgCl_2$, 5 mM Hepes, 2.5 mM $CaCl_2$ and 500 nM tetrodotoxin. The pH was 7.36 when gassed with 95%O_2 and 5% CO_2 at 35 °C. Glass microelectrodes of 2-4 MOhm resistance when filled with potassium acetate (90 mM), KCl (20 mM), $MgCl_2$ (3 mM), Hepes (40 mM), EGTA (3 mM), $CaCl_2$ (1 mM), ATP (2 mM), GTP (0.5 mM), pH adjusted to 7.4 with KOH (1M). Calculated free calcium for this solution was 66 nM (Chelator for Windows 1.1) and series resistance were typically 5 MOhm. Cells were routinely clamped at -20 to -30 mV and hyperpolarised by -30 or -40 mV to generate deactivating tail

currents. Voltage pulses were generated by an amplifier (Axoclamp 2B) in discontinuous mode, while currents were recorded via a signal conditioner (Cyberamp 320), digitised on an ADC (Digidata 1200) and displayed on a PC running commercial software (pClamp 6). All data was stored on optical disk (Panasonic, UK). Data is expressed as mean ± S.E.M. and statistical analysis was performed using an ANOVA and a post hoc Dunnetts test if $p > 0.05$ on the ANOVA.

Membrane currents were recorded from SCG neurons using amphotericin-perforated patch electrodes, as described previously (Selyanko et al., 2002). The composition of the electrode solutions were (mM) for SCG neurons: K acetate 80; KCl 30, HEPES 40, and $MgCl_2$ 3. Solutions were adjusted to pH 7.3-7.4 with KOH and to 280 mOsmol/l with K acetate. Electrode resistances were 2-4 MOhm; access resistances after amphotericin perforation were 6-8 MOhm.

Western blotting

Control and transformed cell membranes were subjected to Western blot analysis to detect the presence of CD38 protein as described previously (Zhong et al., 1997). The membranes were incubated for 2 h with mouse anti-human or -mouse CD38 monoclonal antibody (Immunotech, France and Chemicon Int.), washed 3 times for 5-10 min in a blocking buffer. The membranes were then incubated for 1 h at room temperature in the blocking buffer containing horseradish peroxidase-cojugated goat anti-mouse or anti-rabbit antibodies. The membranes were then washed 3 times for 5-10 min with blocking buffer and reactive proteins visualised with a Western blotting analysis system (Amersham, UK).

Northern blotting

CD38 mRNA was detected using Northern blot analysis. Total cellular RNA was extracted from control NGM1 cells, mock-, and wild-type- or mutant CD38-transfected cells as described previously (Yokoyama et al., 1994). Briefly, 15 μg of total RNA was separated on a 1.1% agarose/2.2 M formaldehyde gel and transferred onto a Zetaprobe nylon membrane. Hybridisation was performed at 42 °C in a solution whose recipe was reported previously (Yokoyama et al., 1994). The probe used was the 0.91-kb *Hind*III/*Spe*I fragment from pZHCD38 labelled by the random primer method. The filter was washed at 50 °C in 0.1 x SSG. Autoradiography was carried out using Fuji BAS1000.

Immunocytochemistry

Control and transfected NG108-15 cells grown on coverslips were washed twice for 3

min with PBS, pH 7.4, fixed for 20 min with freshly prepared 4% formaldehyde in PBS, pH 7.4, at room temperature, and washed 3 times with PBS. The fixed cells were further incubated with 0.1% Triton X-100 in PBS for 5 min; after washing for 3 min (3 times) with PBS, the cells were quenched for 20 min in PBS containing 0.1 M glycine and washed for 5 min with PBS. Immunoreactivity was then demonstrated by incubating the cells with mouse anti-hCD38 mAbs clone T16 (Immunotech, France), which were diluted 1:20 in PBS supplemented with 10% whole goat serum, (12 hr; 4°C), further rinsing 4 times for 3 min in PBS with 10% whole goat serum, followed by incubation with FITC-conjugated goat anti-mouse IgG antibodies diluted 1:200 (1 h; at room temperature). The cells were washed 5 times with PBS and mounted onto glass slides for fluorescence microscope examination.

Calcium measurements

Microspectrofluometric determination of intracellular calcium concentrations ($[Ca^{2+}]_i$) was performed with fura-2 acetoxymethylester (fura-2 AM) as described previously (Hashii et al., 2000). Briefly, the cells were loaded with 5 μM fura-2 AM for 60 min in the dark at 37 °C after an initial DMEM wash. Emission light at 540 nm was monitored via an aperture (10-20 μm in diameter) in response to alternating excitation wavelengths of 340 nm and 380 nm using a Ca^{2+} microspectrofluometrics system (OSP-3, Olympus, Japan).

The inward spread of an increase in $[Ca^{2+}]_i$ by the activation of mAChRs was measured by a confocal microscope as described previously (Akita and Kuba, 2000). Wild or CD38-tranfected cells were loaded with OGB-1 (10 μM) for 2 hours at 37°C. The cells were line-scanned at the rate of 8 msec/sec with Argon laser (488 nm) before, during and after the application of muscarine. The resultant changes in fluorescence were expanded into a X-t plane.

Results

ACh-induced activation of ADP-ribosyl cyclase in SCG

First, we tested whether or not application of ACh induces any changes in ADP-ribosyl cyclase and cADPR hydrolase activities in SCG membranes when measured by [^{3}H]cADPR production (see Methods). In ganglion membranes from 4-week old rats, the mean rate of [^{3}H]cADPR production from [^{3}H]NAD$^+$ was 495.5 $\pm$ 226.9 pmol min^{-1} mg^{-1} of protein (n=4). ACh (100 nM) increased [^{3}H]cADPR formation to 1555.9 $\pm$ 336.7 pmol min^{-1} mg^{-1} of protein (n=4), by 314.0$\pm$ 36.4% ($p < 0.01$), as shown in Fig. 1A. In contrast, cADPR hydrolase activity was negligible in SCG membranes (as with NG108-15 cells: Higashida et al., 1997). This implies that the ACh-induced accumulation of cADPR in the membranes of SCG is due predominantly to accelerated production.

The effect of ACh was confirmed in crude membrane preparations of SCG from 10-35 day old rats using fluorimetric measurement of cyclic GDP-ribose (cGDPR) production as an assay for cADP-ribosyl enzymatic activity (see Methods; Fig. 1B, insert). cGDPR fluorescence increased in a concentration-dependent manner upon exposure to ACh (Fig. 1B). The maximum increase in ADP-ribosyl cyclase was 272.5 ± 28.1% (n=4) of the pre-exposure level was obtained by 10 nM ACh ($p < 0.01$). This increase was prevented by simultaneous application of 0.1 – 10 μM atropine (Fig. 1B open diamond). The action of ACh was replicated by 10 μM carbamylcholine (CCh) (213.7 ± 7.8%, n=3; $p < 0.001$) or 1 μM oxotremorine M (Oxo-M) (256.3 ± 15.5%, n=4; $p < 0.001$).

{Fig. 1 near here}

ADP-ribosyl cyclase stimulation was probably mediated by M1 muscarinic receptors since it was prevented by 100 nM - 10 μM pirenzepine (an M1-selective antagonist; Fig. 2A) but was unaffected by 1 μM AF-DX 116, 4-DAMP or tropicamide (M2, M3 and M4-prefering antagonists, respectively; Fig. 2B).

{Fig. 2 near here}

In order to test whether ADP-ribosyl cyclase stimulation by ACh required receptor coupling to an endogenous G protein, we examined the effect of exogenous GTP in well-washed membranes. Addition of GTP alone (10 - 100 nM) resulted in an increase in enzymatic activity in SCG membrane preparations, increasing basal ADP-ribosyl cyclase activity by 84.2 ± 11.4% (n=6; P <0.01). GTP (10 nM) also enhanced the ACh-induced stimulation (1.5- to 2.5-

fold) of ADP-ribosyl cyclase activity to 341.8 ± 41.4% (n=4; $p < 0.001$). The non-hydrolysable GTP analog, GTP-γ-S, produced a larger increase in basal activity, by 199.3 ± 6.0% (n=3)); under these conditions, however, no further activation by ACh could be observed (as previously noted in neuroblastoma hybrid cells: Higashida et al., 1997).

These results suggest that ADP-ribosyl cyclase activation and cADPR formation, like M current inhibition, is a downstream response of sympathetic neurons to stimulating G protein-coupled M1 muscarinic receptors. We therefore tested whether M current inhibition might be affected in ganglion cells from mice that genetically lack CD38/ADP-ribosyl cyclase (Kato et al., 1999).

Decrease in ACh-induced M-current inhibition in SCG of CD38 knockout mice

First, we compared ADP-ribosyl cyclase activity in wild type ($CD38^{+/+}$) and knockout ($CD38^{-/-}$) mice. As reported previously (Kato et al., 1999; Fukushi et al., 2001), ADP-ribosyl cyclase was greatly reduced in whole homogenate of cells isolated from knockout mouse SCG. Though some remaining activity was detected in the supernatant fraction, activity in the 10,000 x g membrane fraction was barely detectable (< 13%, n=5) (0.18 arbitrary units in $CD38^{-/-}$ *vs* 1.35 units in $CD38^{+/+}$ mice; Fig. 3A). Further, ACh did not increase fluorescence intensity in membrane fractions prepared from SCG from $CD38^{-/-}$ mice, but did increase fluorescence in membranes from $CD38^{+/+}$ mice (Fig. 3B), as in membranes from rat ganglia (cf. Fig.1.)

{Fig. 3 near here}

Armed with this information, we cultured SCG cells from both types of mice for two days, and then measured M currents in individual neurons (Fig. 4). M-currents in ganglion cells from $CD38^{-/-}$ mice were indistinguishable from those in cells from $CD38^{+/+}$ mice. Thus, the mean amplitude of M-current deactivation tails evoked by step hyperpolarization from –20 to –50 mV were 14.1 ± 1.3 (n=17) and 15.9 ±1.5 (n=18) pA pF^{-1} for $CD38^{+/+}$ and $CD38^{-/-}$ mice respectively; see Fig. 4A and B. I-V curves were also comparable (not illustrated). However, the inhibition of the M current induced by 10 μM Oxo-M was dramatically reduced in cells from $CD38^{-/-}$ mice, as shown in Fig. 4B-D, from 74.9 ± 2.1% (n=7) in $CD38^{+/+}$ cells to 28.0 ± 2.2% (n=4) ($p<0.001$) in $CD38^{-/-}$ (Fig. 4D). The time course of development and recovery of M current inhibition was similar in both sets of cells (Fig. 4C).

{Fig. 4 near here}

NGM1 cells over expressing dual cysteine mutant CD38

We next wanted to test the effect of over-expressing the C119K/C201E mutated human CD38/ADP-ribosyl cyclase cDNA, which is devoid of cADPR hydrolase activity and hence functions only as a cADPR synthesizing enzyme (Tohgo et al., 1994; see Introduction). For these experiments we used NGM1 neuroblastoma hybrid cells that has been stably transformed to express the M1 muscarinic acetylcholine receptor (Fukuda et al., 1988). These cells were transfected with a cDNA plasmid encoding the mutated CD38 gene and selected in the presence of 200 $\mu g\ ml^{-1}$ zeocin for 2-6 weeks. The presence of the hCD38 mRNA was verified by Northern blot analysis in zeocin-resistant clones. Expression of the human CD38 protein in the CD38 RNA-positive clones was examined by Western blot analysis using a mouse anti-hCD38 monoclonal antibody (data not shown). Among cells showing a protein band at ~47 kDa for the mutant CD38, three clones designated NGM1-mCD38a, NGM1-mCD38b, and NGM1-mCD38c were selected. Mock- or vector-transformed cells were designated NGM1-V and those transformed with the wild type human CD38, NGM1-CD38.

The efficiency with which the dual cysteine mutant CD38 had been transfected was also confirmed by immunocytochemical analysis (Fig. 5). hCD38-specific immunoreactivity was detected in NGM1-mCD38a, b and c cells (Fig. 5F, H, and J), as in NGM1-CD38 cells (data not shown). Wild type NGM1 or mock-transfected NGM1-V cells showed no or little specific staining under the same conditions (Fig. 5B and D). Our fluorescence microscopic observation did not identify the exact location of the hCD38-immunoreactivity –i.e., whether it was in the cell surface and intracellular membranes or in the perinuclear regions (as shown in MC3T3.E1 CD38-transfected fibroblast cells: Adebanjo et al., 1999). Since thiol-sensitivity of CD38, and its ability to oligomerize have been reported (Grimaldi et al., 1995), we exposed pre-fixed intact cells to 0.5 or 1 mM $HgCl_2$ for 2 min. This resulted in the enhancement of hCD38-specific staining at the plasma membrane area (Fig. 5K). All control (NGM1) or mock-transfected (NGM1-V) cells, as well as hCD38-transfected (NGM1-CD38) cells, possessed endogenous mouse CD38 (Fig. 5L), which was detected with an anti-mouse CD38 monoclonal antibody in Western blot analysis (data not shown).

{Fig. 5 near here}

ADP-ribosyl cyclase activities were studied by [^{3}H]cADPR formation from [^{3}H]NAD^+ as the substrate in all clones tested. The basal cyclase activity in NGM1-mCD38a, b, and c cells was 5.7-, 12.7-, and 12.1-fold higher than that (116 ± 14 pmol min^{-1} mg^{-1} of protein, n=24) of NGM1 cells and 0.74-, 1.64-, and 1.56-fold of that (899 ± 330 pmol min^{-1} mg^{-1} of protein, n=7)

of NG cells, most of which were increased in a clone-specific manner.

The first striking feature in hCD38 transfected cells was the higher rate of [^{3}H]cADPR formation over [^{3}H]ADPR, as shown in their time courses (Fig. 6). In NG control neuroblastoma hybrid cells, NGM1 M1-transformed NG cells and NGM1-V vector-transfected cells, [^{3}H]ADPR formation was much greater than [^{3}H]cADPR production (Fig. 6 A-C), probably due to the endogenous activity of cADPR hydrolase or NAD glycohydrolase (of CD38). Conversely, in C119K/C201E-CD38 transfected NGM1-mCD38a, b, and c cells, [^{3}H]cADPR generation was higher, compared with the conversion rate to [^{3}H]ADPR (Fig. 6D-F). As a cross reference, NGM1-CD38 cells transformed to express wild-type hCD38 with both cyclase and hydrolase activities exhibited the higher [^{3}H]cADPR generation in two clones, but not in other three clones (data not shown). Thus, this clone-specific variation is the reason why we did not used NGM1-CD38 clones in M-current analysis in subsequent experiments.

{Fig. 6 near here}

CCh application to mutant CD38 expressing cells did not produce any activation of ADP-ribosyl cyclase activity, but instead a slight inhibition, to 87-93% of the control level. This was the case in NGM1-CD38 cells with over-expressed wild-type CD38 (data not shown). As shown previously (Higashida et al., 1997), endogenous ADP-ribosyl cyclase activity was increased in M1 mAChR over-expressing NGM1 cells and was inhibited by stimulating endogenous M4 mAChRs in NG cells by 10 μM CCh. The absence of equivalent effects in CD38-transformed cells was not due to loss of M1 mAChRs, because the cells gave clear Ca^{2+} signals on mAChR stimulation (see below). One possibility is that ADP-ribosyl cyclase activity in mutant CD38-transfected cells is mostly derived from the exogenous CD38, which may not be the type of cyclase controlled by mAChRs.

Effect of muscarinic agonists on intracellular calcium in mutant CD38-expressing NGM1 cells

It has previously been shown that ACh produces large transient rises in [Ca^{2+}] in M1 mAChR-transfected NG108-15 cells, as a result of phospholipase C-stimulated $InsP_3$ formation (Fukuda et al., 1988 and 1989). This provides a convenient measure of mAChR stimulation and downstream signaling. All three types of NG cells used in this study possessed comparable levels of resting $[Ca^{2+}]_i$, between 69 and 77 nM. Application of 10 μM CCh elicited an increase to 171 ± 30% (n=9) of the pre-exposure level in NGM1 cells. The same or a greater increase to 286 ± 45% (n=4), 232 ± 16% (n=7) and 251 ± 40% (n=5) was observed in NGM1-

mCD38a, b and c cells, respectively. Hence, receptor activation and downstream signaling were maintained in cells expressing the constitutively-active form of hCD38.

To address the question whether the intracellular distribution of the ACh-induced Ca^{2+} rise in C119K/C201E-CD38 over-expressing cells differed from that in control cells, we applied digital imaging analysis by confocal microscopy. Line scans were made in mutant CD38 over-expressing cells or wild-type NG cells loaded with the Ca^{2+} indicator, OGB-1, after local application of 100 μM muscarine. Although the magnitude of the rise was greater in NGM1-mCD38b cells, the elevation of $[Ca^{2+}]_i$ started from the submembrane compartment beneath the point of application and then spread at the same rate into the deeper regions in both NGM1 and NGM1-mCD38b cells. Thus, the topographical distribution of the sites of Ca^{2+} release was unchanged by the over-expression of mutated CD38.

Carbachol-induced biphasic membrane current response

CCh, when applied to parental NGM1 cells, produces an outward current due to the opening of Ca^{2+}-dependent K^+ channels, followed by an inward current caused principally by suppression of M-current (Fukuda et al., 1988; Robbins et al, 1992: Higashida et al., 1995, 1996). We therefore examined how these two CCh-induced current changes were modified in cells over-expressing mutant CD38.

Focal application of 3 µl of 10 µM CCh to the external surface of NGM1-mCD38a, b, and c cells voltage-clamped at -20 mV, produced either a similar biphasic current response to that in wild-type cells (Fig.7A), or a large inward current with a negligible initial outward current (Fig.7B). The mean outward current elicited by CCh in NGM1-mCD38a, b, and c cells appeared somewhat smaller than that in NGM1 and NGM1-V cells (Fig. 8A), whereas the mean inward current was similar or somewhat larger (Fig. 8B).

{Figs. 7 and 8 near here}

Inhibition of the M-like current $I_{K(M,ng)}$ (Robbins et al., 1992) at the peak of the second-phase inward current following local application of 3 µl of 10 µM acetylcholine (to give an estimated equilibrium concentration of 15 nM) was measured from the reduction in the amplitude of the deactivation relaxations that accompanied 20 mV hyperpolarizing steps from the holding potential of -20 mV (Fig.7A, B, lower records) The average inhibition in NGM1 and NGM1-V cells was 32.1 ± 6.5% (n=18) and 26.3 ± 4.7% (n=19), similar to that previously reported (Higashida et al, 1996). In contrast, the same treatment in NGM1-mCD38a, b and c cells produced significantly larger inhibitions ($p < 0.001$) up to 83.2 ± 12.9% (n=5), 80.3 ±

3.6% (n=23), and 80.8 ± 6.2% (n=8), respectively (Fig. 8C). Judging from the dose-response relationship obtained by perfusion of various concentrations of ACh (Fig. 9), the IC_{50} of ACh was calculated to be about 1.55 and 0.88 μM ACh for NGM1-mCD38b and c cells, compared with 13 μM for wild-type NGM1 cells.

{Fig. 9 near here}

Finally, we examined whether the voltage-dependent characteristics of M currents, *per se*, were altered in mutant CD38 expressing cells. Therefore control (NGM1), mock-transfected (NGM1-V) and the dual cysteine mutant CD38 transfected cells (NGM1-mCD38b) were recorded under identical conditions to measure $I_{K(M,ng)}$ in the whole-cell voltage-clamp mode. The total amplitude of the deactivation relaxation measured at -50 mV after a step from -20 mV was found to be not significantly different between the three cell types. Construction of an activation curve followed by a fit to a Boltzman function (see Robbins et al., 1992) demonstrated no significant difference between the half activation potential (Vo) or the slope value (s) among all three groups of cells (Table 1). Construction of a time constant-Vm curve (Robbins et al., 1992) also indicated no significant difference between the opening (αo) or closing (βo) rate constants or the slope factor (c). Thus, over-expression of the mutated CD38 had little effect on the gating, voltage dependence or kinetics of the channels responsible for $I_{K(M,ng)}$. [Note: for these analyses, a composite time-constant embracing both components of $I_{K(M,ng)}$ current relaxation (see Meves et al., 1999; Selyanko et al., 1999) were applied (see Robbins et al., 1992). The fact that this composite time-constant was unchanged implies that the two components of current carried by KCNQ and ERG channels were affected equally.]

{Table 1 near here}

Discussion

The results of previous experiments (see Introduction) have indicated that cADPR may play a role in inhibition of the M-like current in NG108-15 neuroblastoma hybrid cells that results from M1 mAChR stimulation. In this report we have investigated this possibility further by the unique approach of genetically manipulating the enzyme that may be responsible for generating cADPR, human CD38. This has led to two significant advances.

First, over-expression of a mutated form of the cADPR synthetic enzyme, CD38 /ADP-ribosyl cyclase, that was devoid of hydrolase activity (and therefore acts as a constitutively-active ADP-ribosyl cyclase, leading to higher levels of cADPR) strongly augmented the

inhibition of the M-like current in NG108-15 cells. This was specific to this component of M1-mAChR action since there was no corresponding increase in the initial elevation of intracellular Ca^{2+} or in the consequential outward current mediated by activation of Ca^{2+}-dependent K^+ channels (see Higashida & Brown, 1986; Brown & Higashida, 1988; Robbins et al., 1991 and 1993). Interestingly (and in contrast to control cells: Higashida et al., 1997), activation of the M1 receptors did not appear to enhance the activity of this mutated CD38 enzyme. Hence, the enhanced inhibition of the M-like current appears to result from the higher overall basal rate of ADP-ribosyl cyclase activity.

Second – and perhaps more significantly – we have extended the putative role for cADPR in M current regulation to include primary sympathetic neurons. Thus, we have shown that ACh accelerates the synthetic activity of ADP-ribosyl cyclase in membrane preparations from sympathetic ganglia, just as it does in NG108-15 cell membranes (Higashida et al., 1997). Tests with antagonists showed that this was due to stimulation of endogenous M1 mAChRs, and tests with GTP and GTP-γ-S indicated that it resulted from M1 mAChR–G protein coupling.

Finally, using CD38 knock-out mice, in which negligible ADP-ribosyl cyclase activity could be detected in the membrane fractions prepared from sympathetic ganglia, we found a very substantial reduction in the mAChR-induced inhibition of the native M currents in dissociated sympathetic neurons in $CD38^{-/-}$ mice when compared with that in neurons from wild-type $CD38^{+/+}$ mice, from ~75% to ~25%.

Some of the experimental manipulations previously used to investigate the role of cADPR in neuroblastoma cells – for example, intracellular dialysis of cADPR and its antagonists – are difficult to apply to sympathetic neurons because of the rapid M current 'rundown' usually experienced with whole-cell recording (see, for example, Brown et al., 1995). This has hitherto precluded extension of information drawn from NG108-15 cells to primary neurons. The present experiments are therefore particularly important in suggesting that such an extension can reasonably be made.

Nevertheless, when viewing cADPR as a potential 'second messenger' for M current inhibition (see further below), a number of questions remain. First, CD38 is a multifunctional ectoenzyme (Shubinsky and Schlesinger, 1997), which generates cADPR from β-NAD^+ in the extracellular compartment. This conflicts with the established dogma that second messengers are generated and remain intracellularly (with the exception perhaps of nitric oxide). This apparent anomaly might be explained in a number of ways. First, perhaps it is extracellular cADPR that modulates the M-current. This seems unlikely, because cADPR has been shown to inhibit the neurobastoma current when applied intracellularly via the patch-pipette (Higashida et al., 1995) and its antagonists are also effective from the inside (Bowden et al., 1999). Second,

it has been suggested that some of the CD38 protein may exist on intracellular membranes and therefore generate cADPR within the cell (Kato et al., 1995; Chini et al., 2002; Khoo and Chang, 2002). Thirdly it has been proposed by Zocchi et al. (1999) that plasma membrane-located CD38 internalises β-NAD^+ into vesicles and, following conversion of β-NAD^+ to cADPR, pumps cADPR into the cytosol. Similar considerations apply to the proposed involvement of cADPR in other cellular responses such as fertilization, insulin secretion and cardiac contraction (Galione et al., 1993: Lee et al., 1993;Takasawa et al., 1993a; Higashida et al., 1999, 2000b) and clearly need resolution.

Second, the *modus operandi* of cADPR as a potential M current inhibitor is not yet clear. The most widely-accepted view is that it acts by facilitating ryanodine receptor-induced intracellular Ca^{2+} release (Meszaros et al., 1993; Lee et al., 1994; Thomas et al., 2001). However, in previous experiments, no evidence could be adduced to support a role for either Ca^{2+} (Higashida et al., 1995) or ryanodine receptors (Bowden et al., 1999) in the regulation of the M-like currents in neuroblastoma hybrid cells. Equally, an alternative possibility – that of a direct effect on the M channels themselves – can be excluded because cADPR did not affect M channel activity when applied to the inside face of excised membrane patches from sympathetic neurons (Bowden et al., 1999).

Notwithstanding this paucity of mechanistic information, the experimental evidence for cADPR as a putative 'second messenger' for G protein-coupled receptor-induced M current inhibition now appears quite substantial (see Introduction), and comparable to that for some other suggested messengers such as Ca^{2+} and protein kinase C (see Marrion, 1997). Recent work has added phosphatidylinositol bisphosphate (PIP_2) depletion to that list of putative second messenger systems (Suh & Hille, 2002). One possibility that emerges is that changes in membrane phosphatidylinositide levels provide the unifying mechanism underlying the regulation of M channels by Gq/11-coupled receptors in general, but that other modulators generated by receptor stimulation enhance the sensitivity of the channels to changes in PIP_2 levels in a receptor-specific manner. Thus, for bradykinin B2 receptors (Cruzblanca et al., 1998) and nucleotide P2Y receptors (Bofill-Cardona et al., 2000), closure is facilitated by the $InsP_3$-induced rise in Ca^{2+} (perhaps resulting from a close proximity of the transmitter receptors to the $InsP_3$-receptors: Delmas et al., 2002) and the consequent effect of Ca^{2+} on channel activity (Selyanko & Brown, 1996). On the other hand, formation of diacylglycerol and consequent activation of protein kinase C bound to the A-kinase anchoring protein (AKAP) in a complex with the M channel acts as a sensitizer for mAChR-mediated inhibition (Hoshi et al., 2003). The present results strongly suggest that ADP-ribosyl cyclase activation, and consequential formation of cADPR, also falls into this category of 'sensitizing mechanisms'.

An essential requirement for future research is to determine more precisely the interactions between the various regulatory mechanisms for these channels.

References

Adebanjo OA, Anandatheerthavarada HK, Koval, AP, Moonga BS, Biswas G, Sun L, Sodam BR, Benis PJR, Huanh C L-H, Epstein S, Lai FA, Avadhani NG, Zaid M (1999) A new function for CD38/ADP-ribosyl cyclase in nuclear Ca^{2+} homeostasis. Nature Cell Biol 1: 409-414.

Akita T, Kuba K (2000) Functional triads consisting of ryanodine receptors, Ca^{2+} channels, and Ca^{2+}-activated K^+ channels in bullfrog sympathetic ganglion neurons; Plastic modulation of action potentials. J Gen Physiol 116: 697-720.

Bofill-Cardona E, Vartian N, Nanoff C, Freissmuth M, Boehm S (2000) Two different signaling mechanisms involved in the excitation of rat sympathetic neurons by uridine nucleotides. Mol Pharmacol 57: 1165-1172.

Bowden SEH, Selyanko AA, Robbins J (1999) The role of ryanodine receptors in the cyclic ADP ribose modulation of the M-like current in rodent m1 muscarinic receptor-transfected NG108-15 cells. J Physiol (Lond) 519: 23-34.

Brown DA, Higashida H (1988) Membrane current responses of NG108-15 mouse neuroblastoma x rat glioma hybrid cells to bradykinin.J Physiol (Lond) 397: 167-184.

Brown, DA, Buckley NJ, Caulfield MP, Duffy SM, Jones S, Lamas JA, Marsh SJ, Robbins J, Selyanko AA. (1995). Coupling of muscariic acetylcholine receptors to neural ion channels: closure of K^+ channels. In: Molecular mecahnisms of muscarinic acetylcholine receptor function (Wess J, ed), pp165-182.New York: Springer.

Chavis P, Fagni I, Lansmann JB, Bockaert J (1996) Functional coupling between ryanodine receptors and L-type calcium channels in neurons. Nature 328: 719-722.

Chini EN, Chini CS, Kato I, Takasawa S, Okamoto, H (2002) CD38 is the major enzyme responsible for synthesis of nicotinic acid-adenine dinucleotide phosphate in mammalian tissues. Biochem J 362: 125-130.

Cruzblanca H, Koh DD, Hille B (1998) Bradykinin inhibits M current via phospholipase C and

Ca^{2+} release from IP_3-sensitive Ca^{2+} stores in rat sympathetic neurons. Proc Natl Acad Sci USA 95: 7151-7156.

Davies PJ, Ireland DR, McLachlan EM (1996) Sources of Ca^{2+} for different Ca^{2+}-activated K+ conductances in neurones of the rat superior cervical ganglion. J Physiol (Lond) 495: 353-366.

Delmas P, Brown DA (2002) Junctional signaling microdomains: bridging the gap between the neuronal cell surface and Ca^{2+} stores. Neuron 36: 787-790.

Empson RM, Galione A (1997) Cyclic ADP-ribose enhances coupling between voltage-gated Ca^{2+} entry and intracellular Ca^{2+} release. J Biol Chem 272: 20967-20970.

Fukuda K, Higashida H, Kubo T, Maeda A, Akiba I, Bujo H, Mishina M, Numa S (1988) Selective coupling with K^+ currents of muscarinic acetylcholine receptor subtypes in NG108-15 cells. Nature 335: 355-358.

Fukuda K, Kubo T, Maeda A, Akiba I, Bujo H, Nakai J, Mishina M, Higashida H, Neher E, Marty A, Numa S (1989) Selective effector coupling of muscarinic acetylcholine receptor subtypes. Trends Pharmacol Sci 10 Suppl: 4-10.

Fukushi Y, Kato I, Takasawa S, Sasaki T, Ong BH, Sato M, Ohsaga A, Sato K, Shirato K, Okamoto H, Maruyama Y (2001) Identification of cyclic ADP-ribose-dependent mechanisms in pancreatic muscarinic Ca^{2+} signaling using CD38 knockout mice. J Biol Chem 276: 649-655.

Graeff RM, Walseth TF, Fryxell K, Branton WD, Lee HC (1994) Enzymatic synthesis and characterisations of cyclic GDP-ribose. A procedure for distinguishing enzymes with ADP-ribosyl cyclase activity. J Biol Chem 269: 30260-30267.

Grimaldi JC, Balasubramanian S, Kabra NH, Shanafelt A, Bazan JF, Zurawski G, Howard MC (1995) CD38-mediated ribosylation of proteins. J Immunol 155: 811-817.

Galione A, McDougall A, Busa WB, Willmott N, Gillot I, Whitaker M (1993) Redundant mechanisms of calcium-induced calcium release underlying calcium waves during fertilization of sea urchin eggs. Science 261: 348-351.

Harada N, Santos-Argumedo L, Chang R, Grimaldi JC, Lund FE, Brannan CI, Copeland NG, Jenkins NA, Heath AW, Parkhouse RM, Howard M (1993) Expression cloning of a cDNA encoding a novel murine B cell activation marker. Homology to human CD38.
J Immunol 151: 3111-3118.

Hashii M, Minabe Y, Higashida H (2000) cADP-ribose potentiates cytosolic Ca^{2+} elevation and Ca^{2+} entry via L-type voltage-activated Ca^{2+} channels in NG108-15 neuronal cells. Biochem J 345: 207-215.

Higashida H, Brown DA (1986) Two polyphosphatidylinositide metabolites control two K^+ currents in a neuronal cell. Nature 323: 333-335.

Higashida H, Brown DA, Robbins J (2000a) Both linopirdine- and WAY123,398-sensitive components of $I_{K(M,\ ng)}$ are modulated by cADP ribose in NG108-15 cells. Pflugers Arch 441: 228-234.

Higashida H, Egorova A, Hoshi N, Noda M (1996) Streptozotocin, an inducer of NAD^+ decrease, attenuates M-potassium current inhibition by ATP, bradykinin, angiotensin II, endothelin 1 and acetylcholine in NG108-15 cells. FEBS Lett 379: 236-238.

Higashida H, Egorova A, Higashida C, Zhong ZG, Yokoyama S, Noda M, Zhang JS (1999) Sympathetic potentiation of cyclic ADP-ribose formation in rat cardiac myocytes.
J Biol Chem 274: 33348-33354.

Higashida H, Hashii M, Yokoyama S, Hoshi N, Asai K, Kato T (2001a) Cyclic ADP-ribose as a potential second messenger for neuronal Ca^{2+} signaling. J Neurochem 76: 321-331.

Higashida H, Hashii M, Yokoyama S, Hoshi N, Chen X-L, Egorova A, Noda M, Zhang J-S (2001b) Cyclic ADP-ribose as a second messenger revisited from a new aspect of signal transduction from receptors to ADP-ribosyl cyclase. Pharmacol Therap 90: 283-296.

Higashida H, Robbins J, Egorova A, Noda M, Taketo M, Ishizaka N, Takasawa S, Okamoto H, Brown DA (1995) Nicotinamide-adenine dinucleotide regulates muscarinic receptor-coupled K^+ (M) channels in rodent NG108-15 cells. J Physiol (Lond) 482: 317-323.

Higashida H, Streaty RA, Klee W, Nirenberg M (1986) bradykinin-activated transmembrane signals are coupled via No or Ni production of inositol 1,4,5-trisphosphate, a second messenger in NG108-15 neuroblastoma-glioma hybrid cells. Proc Natl Acad Sci USA 83: 942-946.

Higashida H, Yokoyama S, Hashii M, Taketo M, Higashida M, Takayasu T, Ohshima T, Takasawa S, Okamnoto H, Noda M (1997) Muscarinic receptor-mediated dual regulation of ADP-ribosyl cyclase in NG108-15 neuronal cell membranes. J Biol Chem 272: 31272-31277.

Higashida H, Zhang J-S, Hashii M, Shintaku M, Higashida C,Takeda Y (2000b) Angiotensin II stimulates cyclic ADP-ribose formation in neonatal rat cardiac myocytes. Biochem J 352: 197-202.

Hoshi N, Zhang J-S, Omaki M, Takeuchi T, Yokoyama S, Wanaverbecq N, Langeberg LK, Yoneda Y, Scott JD, Brown DA, Higashida H. (2003). AKAP150 signaling complex promotes suppression of the M-current by muscarinic agonists. Nat Neurosci (in press).

Hua SY, Tokimasa T, Takasawa S, Furuya Y, Nohmi M, Okatomo H, Kuba K (1994) Cyclic ADP-ribose modulated Ca^{2+} release channels for activation by physiological Ca^{2+} entry in bullfrog sympathetic neurons. Neuron 12: 1073-1079.

Jackson DG, Bell JL (1990) Isolation of a cDNA encoding the human CD38 (T10) molecule a cell surface glycoprotein with an unusual discontinuous pattern of expression during lymphocyte differentiation. J Immunol 144: 2811-2815.

Kato I, Takasawa S, Akabane A, Tanaka O, Abe H, Takamura T, Suzuki Y, Nata K, Yonekura H, Yoshimoto T, Okamoto H (1995) Regulatory role of CD38 (ADP-ribosyl cyclase/cyclic ADP-ribose hydrolase) in insulin secretion by glucose in pancreatic β cells. J Biol Chem 270: 30045-30050.

Kato I, Yamamoto Y, Fujimura M, Noguchi N, Takasawa S, Okamoto H (1999) CD38 disruption impairs glucose-induced increases in cyclic ADP-ribose, $[Ca^{2+}]_i$, and insulin secretion. J Biol Chem 274: 1869-1872.

Khoo KM,Chang CF (2002) Identification and characterisation of nuclear CD38 in the rat

spleen. Int J Biochem Cell Biol 34: 43-54.

Kim H, Jacobson EL, Jacobson MK (1993) Synthesis and degradation of cyclic ADP-ribose by NAD glycohydrolases. Science 261: 1330-1333.

Koguma T, Takasawa S, Tohgo A, Karasawa T, Furuya Y, Yonekura H, Okamoto H (1994) Cloning and characterization of cDNA encoding rat ADP-ribosyl cyclase/cyclic ADP-ribose hydrolase (homologue to human CD38) from islets of Langerhans. Biochim Biophys Acta 1223: 160-162.

Lee HC (1997) Mechanisms of calcium signaling by cyclic ADP-ribose and NAADP. Physiol Rev 77: 1133-1164.

Lee HC (2001) Physiological functions of cyclic ADP-ribose and NAADP as calcium messengers. Annu Rev Pharmacol Toxicol 41: 317-345.

Lee HC, Aarhus R, Graeff R, Gurnack ME, Walseth TF (1994) Cyclic ADP ribose activation of the ryanodine receptor is mediated by calmodulin. Nature 370: 307-309.

Lee HC, Aarhus R, Walseth TF (1993) Calcium mobilization by dual receptors during fertilization of sea urchin eggs. Science 261: 352-354.

Marrion NV (1997) Control of M-current. Ann Rev Physiol 59: 483-504.

Mészáros LG, Bak J, Chu A (1993) Cyclic ADP-ribose as an endogenous regulator of the non-skeletal type ryanodine receptor Ca^{2+} channel. Nature 364: 76-79.

Meves H, Schwarz JR,Wulfsen I. (1999) Separation of M-like current and ERG current in NG108-15 cells. Br J Pharmacol 127: 1213-1223.

Prasad GS, McRee DE, Stura EA, Levitt DG, Lee HC, Stout CD (1996) Crystal structure of Aplysia ADP ribosyl cyclase, a homologue of the bifunctional ectozyme CD38. Nat Struct Biol 3: 957-964.

Robbins J, Caulfield MP, Higashida H, Brown DA (1991) Genotypic m3-muscarinic receptors

preferentially inhibit M-currents in DNA-transfected NG108-15 neuroblastoma x glioma hybrid cells. Eur J Neurosci 3: 820-824.

Robbins J. Marsh SJ Brown DA (1993) On the mechanism of M-current inhibition by muscarinic m1 receptors in DNA-transfected rodent neuroblastoma x glioma cells. J Physiol (Lond) 469: 153-178.

Robbins J, Trouslard J, Marsh SJ, Brown DA (1992) Kinetic and pharmacological properties of the M-current in rodent neuroblastoma x glioma hybrid cells. J Physiol (Lond) 451: 159-185.

Selyanko AA, Brown DA (1996) Regulation of M-type potassium channels in mammalian sympathetic neurons: action of intracellular calcium on single channel currents. Neuropharmacol 35: 933-947.

Selyanko AA, Hadley JA, Wood IC, Abogadie FC, Delmas P, Buckley NJ, London B, Brown DA (1999) Two types of K^+ channel subunit, Erg1 and KCNQ2/3, contribute to the M-like current in a mammalian neuronal cell. J Neurosci 19: 7742-7756.

Selyanko AA, Delmas P, Hadley JK, Tatulian L, Wood IC, Mistry M, London B, Brown DA (2002) Dominant-negative subunits reveal potassium channel families that contribute to M-like potassium currents J Neurosci 22: RC212.

Shubinsky G, Schlesinger M (1997) The CD38 lymphocyte differentiation marker: new insight into its ectoenzymatic activity and its role as a signal transducer. Immunity 7: 315-324.

States DJ, Walseth TF, Lee HC (1992) Similarities in amino acid sequences of aplysia ADP-ribosyl cyclase and human lymphocyte antigen CD38. Trends Biochem Sci 17: 495.

Suh B-C, Hille B (2002) Recovery from muscarinic modulation of M current channels requires phosphatidylinotitol 4,5-bisphosphate synthesis. Neuron 35: 507-520.

Summerhill RJ, Jackson DG, Galione A (1993) Human lymphocyte antigen CD38 catalyzes the production of cyclic ADP-ribose. FEBS Lett 335: 231-233.

Takasawa S, Nata K, Yonekura H, Okamoto H (1993a) Cyclic ADP-ribose in insulin secretion

from pancreatic β cells. Science 259: 370-373.

Takasawa S, Tohgo A, Noguchi N, Koguma T, Nata K, Sugimoto T, Yonekura H, Okamoto H (1993b) Synthesis and hydrolysis of cyclic ADP-ribose by human leukocyte antigen CD38 and inhibition of the hydrolysis by ATP. J Biol Chem 268: 26052-26054.

Thomas JM, Masgrau R, Churchill GC, Galione A (2001) Pharmacological characterization of the putative cADP-ribose receptor. Biochem J 359: 451-457.

Tohgo A, Takasawa S, Noguchi N, Koguma T, Nata K, Sugimoto T, Furuya Y, Yonekura H, Okamoto H (1994) Essential cysteine residues for cyclic ADP-ribose synthesis and hydrolysis by CD38. J Biol Chem 269: 28555-28557.

Wang HS, Pan Z, Shi W, Brown BS, Wymore RS, Cohen IS, Dixon JE, McKinnon D (1998) KCNQ2 and KCNQ3 potassium channel subunits: molecular correlates of the M-channel. Science 282: 1890-1893.

Yokoyama S, Kimura Y, Taketo M, Black JA, Ransom BR, Higashida H (1994) B2 bradykinin receptors in NG108-15 cells: cDNA cloning and functional expression. Biochem Biophys Res Commun 200: 634-641.

Zhong ZG, Yokoyama S, Noda M, Higashida H (1997) Overexpression of adhesion molecule L1 in NG108-15 neuroblastoma x glioma hybrid cells enhances dibutyryl cyclic AMP-induced neurite outgrowth and functional synapse formation with myotubes. J Neurochem 68: 2291-2299.

Zocchi E, Usai C, Guida L, Franco L, Bruzzone S, Passalaqua M, De Flora A (1999) Ligand-induced internalisation of CD38 results in intracellular Ca^{2+} mobilization: role of NAD^{+} transport across cell membranes. FASEB J 13: 273-283.

Table 1. Amplitude and kinetic properties of $I_{K(M,ng)}$ in control and cysteine mutated CD38-transfected NGM1 cells.

Parameter	NGM1 (n=9)	NGM1-V (n=8)	NGM1-mCD38b (n=9)
Amplitude (pA)	524 ± 85	1272 ± 408	700 ± 127
Vo (mV)	-38.9 ± 1.61	-36.3 ± 1.5	-38.5 ± 0.5
s	-7.7 ± 1.6	-6.5 ± 0.6	-6.8 ± 0.5
αo (s-1)	1.9 ± 0.4	1.1 ± 0.2	1.0 ± 0.2
βo (s-1)	1.4 ± 0.1	1.2 ± 0.1	1.2 v 0.2
C (mV)	15.0 ± 0.8	15.9 ± 0.6	15.5 ± 0.6

Biophysical properties of $I_{K(M,ng)}$ in control (NGM1), vector transfected (NGM1-V) cells and dual cysteine mutant CD38 (NGM1-mCD38b) cells. Data are given as the mean ± s.e.m. for the deactivation tail amplitude at -50 mV, half activation potential (Vo), slope (s) obtained from activation curves fit by Boltzman equation $G/Gmax = 1/\{1+expV_{2/1}[(Vo-Vc)/s]\}$. The opening (αo) and closing (βo) rate constants were calculated from tau-Vc curve fit by the equations $\alpha = \alpha o \exp((Vc-Vo)/C)$ and $\beta = \beta o((Vc-Vo)/-C)$. Number of cells is given in brackets.

Figure legends

Fig. 1. Activation of ADP-ribosyl cyclase by ACh in rat SCG. A. ADP-ribosyl cyclase was measured from the initial velocity during 2 min with membranes prepared from rat SCG. Values were calculated by conversion of [^{3}H]cADPR from [^{3}H]NAD$^+$ in the presence or absence of 100 nM ACh in 4 experiments. Values indicate mean ± S.E.M. * indicates significantly different from the control at $p < 0.01$. B. Relationship between ACh concentration and ADP-ribosyl cyclase activity with (open diamonds) or without 1 μM atropine (filled circles) measured fluorometrically. The fluorescence of the resulting cGDPR was continuously monitored before and after application of 100 nM ACh (arrow), as shown in insert. Changes in velocity were plotted. Data represent the mean (± S.E.M.) in 3-5 measurements. Some S.E.M. values are within the size of symbols. * and ** significantly different from the value with atropine at the indicated ACh concentrations at $p < 0.001$ and 0.01, respectively. *Insert,* Bars indicate 30 s and 0.1 arbitrary unit.

Fig. 2. Effects of subtype-specific antagonists on ACh-induced activation of ADP-ribosyl cyclase activity in rat SCG. A. Relationship between ACh concentration and ADP-ribosyl cyclase activity with (open squares) or without 1 μM pirenzepine (filled circles) measured fluorometrically. Values indicate mean ± S.E.M. in 3-5 measurements. * significantly different from the value with pirenzepine at the indicated ACh concentrations at $p < 0.01$. B. Effects of 4 subtype-specific antagonists at 1 μM on ACh (100 nM)-induced activation of ADP-ribosyl cyclase. Values indicate mean ± S.E.M. in 3-5 measurements. * significantly different from control value at $p < 0.001$.

Fig. 3. Synthesis of cGMP-ribose and dose-dependent effect of ACh in SCG membranes of CD38 $^{+/+}$ wild type and CD38 $^{-/-}$ knockout mice. cGDPR synthesis was measured flourometrically. A. Membrane preparations of SCG of CD38$^{+/+}$ and CB38$^{-/-}$ mice were incubated for 700s and basal activities (arbitrary units min^{-1} mg protein^{-1}) were calculated. * significantly different from the value of wild type mice at $p < 0.001$ (n=7). B. Membranes were incubated with different concentrations of ACh and the velocity was calculated. Results are expressed as percentage of control rate of cGDP-ribose in 4 independent experiments. * and ** significantly different from values at the indicated ACh concentrations in CD38$^{-/-}$ mice at $p <$ 0.002 and 0.001 respectively.

Fig. 4. Comparison of M-current inhibition in cultured SCG neurons of wild-type CD38$^{+/+}$ or CD38$^{-/-}$ mutant mice. Typical current responses to a voltage step to –50 mV from holding

potential of –30 mV for M currents in $CD38^{+/+}$ (A) or $CD38^{-/-}$ (B) mice before (trace 1) during (2) and after (3) application of 10 μM Oxo-M. C and D. Statistical evaluation of the effect of Oxo-M on M-current in both types of mice. Depicted are the amplitudes of M-current deactivation relaxations in response to the voltage steps in A and B and inhibition of M-current. Means ± S.E.M. from between 4 and 7 experiments in $CD38^{+/+}$ and $CD38^{-/-}$ mice. *significantly different at $p < 0.005$.

Fig. 5. Immunofluorescence of human or mouse CD38 in various types of cells derived from NGM1 cells. Using a fluorescence microscopy, FITC for NGM1, (A, B), NGM1-V (C, D), NGM1-mCD38a (E, F), NGM1-mCD38b (G, H), and NGM1-mCD38c (I, J and K) cells. Images obtained with (B, D, F, H, J, and K) or without (A, C, E, G and I) anti-human CD38 mouse monoclonal antibody. (magnification, x756). In K, the cells were treated with 1 mM $HgCl_2$ for 2 min in order to facilitate membrane localization. L, immunofluoresence of endogenous CD38 obtained with anti-mouse CD38 monoclonal antibody in NGM1. Note that fluorescence is seen in cell membrane and processes. (magnification, x1512).

Fig. 6. Time course of ADP-ribosyl cyclase activity in membranes prepared from various types of NG108-15 cells. Aliquots (20 μl) containing 1.5-4.5 μg of membrane protein of NG (A), NGM1 (B), NGM1-V (C), NGM1-mCD38a (D), NGM1-mCD38b (E), and NGM1-mCD38c (F) cells were incubated for the indicated time (0-2 min). Radioactivity in spots corresponding to authentic cADPR (filled circle) and ADPR (open square) on TLC sheets was measured. Each data point represents the mean of two independent experiments.

Fig. 7. M-current suppression in two NGM1-mCD38b cells. Top, inward current response to focal application of CCh (3 μl, 10 μM), being associated with (A) or without (B) initial outward current. Repetitive hyperpolarization step pulses (-20 mV, 1 s) were applied to estimate the conductance and M current from a holding membrane potential of -20 mV (Middle). Bottom, Expanded records of current transients evoked by ach -20 mV step pulse. They were obtained at the time gap in the top trace. Left (a), before applying CCh; centre (b), during the inward current; right (C and D), after full or over recovery.

Fig. 8. ACh-induced outward and inward currents and inhibition of M current in various types of cells derived from NGM1 cells. Histograms show the average amplitude of outward (A) and inward (B) currents induced by focal application of 100 μM CCh (3 μl) in cells indicated on left. C shows the average amount of inhibition of $I_{K(NG, M)}$ recorded in cells as

described in Fig. 4D. Number of cells tested ranged from 5 to 6. Bars, S.E.M. $*p < 0.001$ from two control cells.

Fig. 9. The concentration-dependent inhibition of M-current by acetylcholine in NGM1 (filled circle), NGM1-mCD38b (open square) and NGM1-mCD38c (open diamond) cells. The relative inhibition of the M-current deactivation relaxations produced by the increasing concentration of ACh in three different subclones was plotted. Relative $I_{K(M,ng)}$ was calculated by dividing the amplitude prior to application with that obtained after the perfusion of the indicated concentrations of ACh. Each point represents the mean (±S.E.M.) of 4-5 cells.

Figure 1

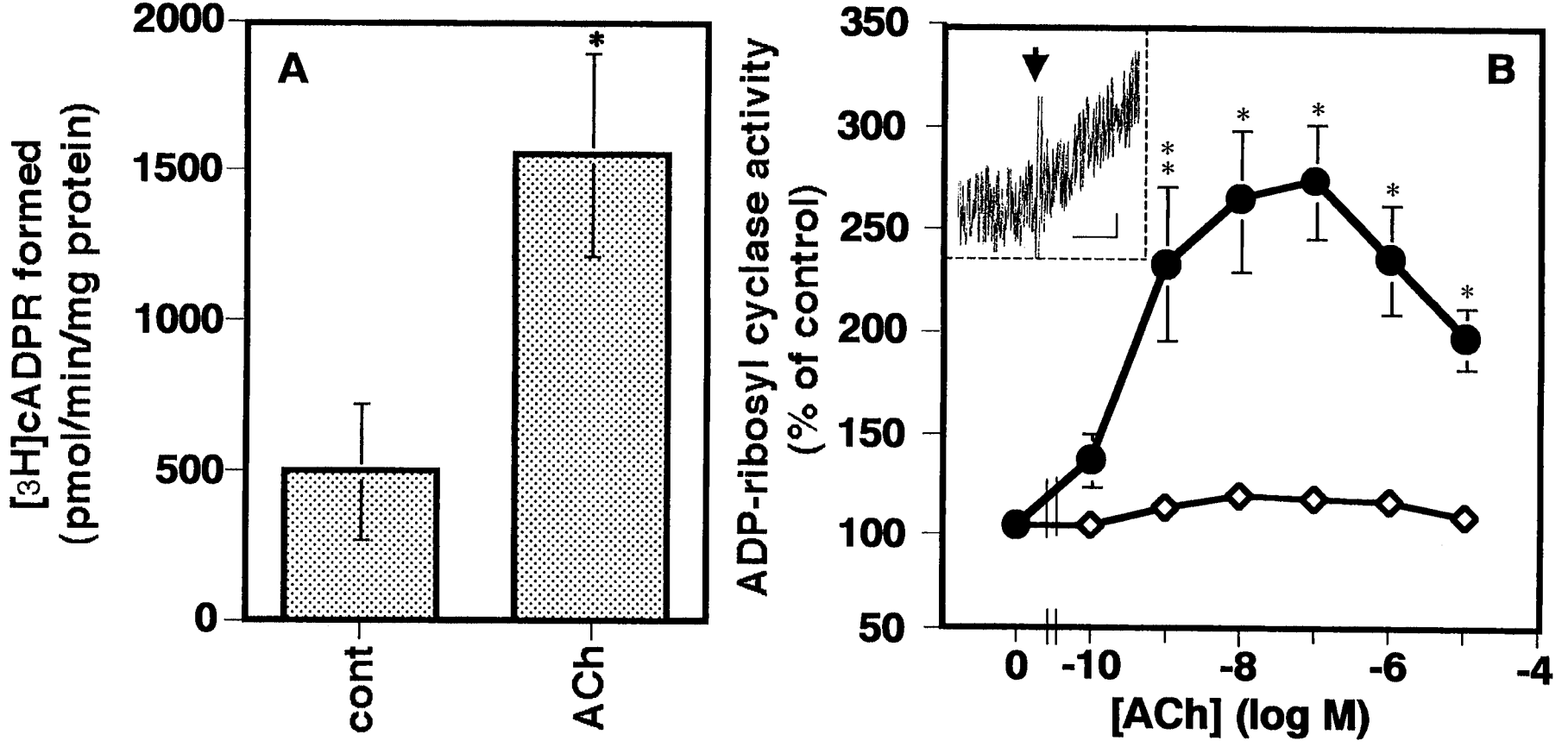
A
[3H]cADPR formed
(pmol/min/mg protein)
2000
1500
1000
500
0
cont
ACh
*
B
ADP-ribosyl cyclase activity
(% of control)
350
300
250
200
150
100
50
0
-10
-8
-6
-4
[ACh] (log M)
**
*
*
*
*

Figure 2

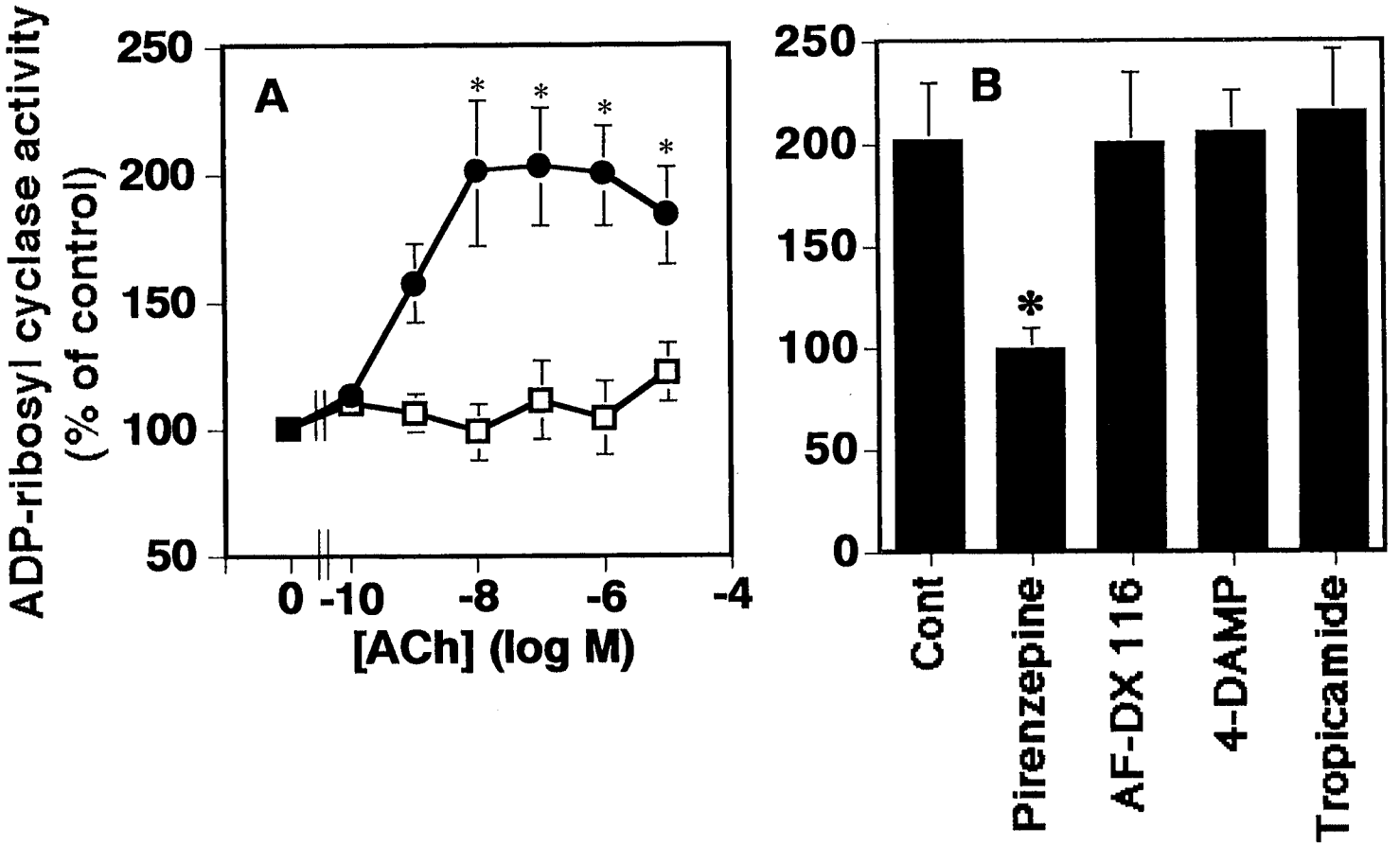
ADP-ribosyl cyclase activity
(% of control)
250
200
150
100
50
A
*
*
*
*
0
-10
-8
-6
-4
[ACh] (log M)
250
200
150
100
50
0
B
*
Cont
Pirenzepine
AF-DX 116
4-DAMP
Tropicamide

Figure 3

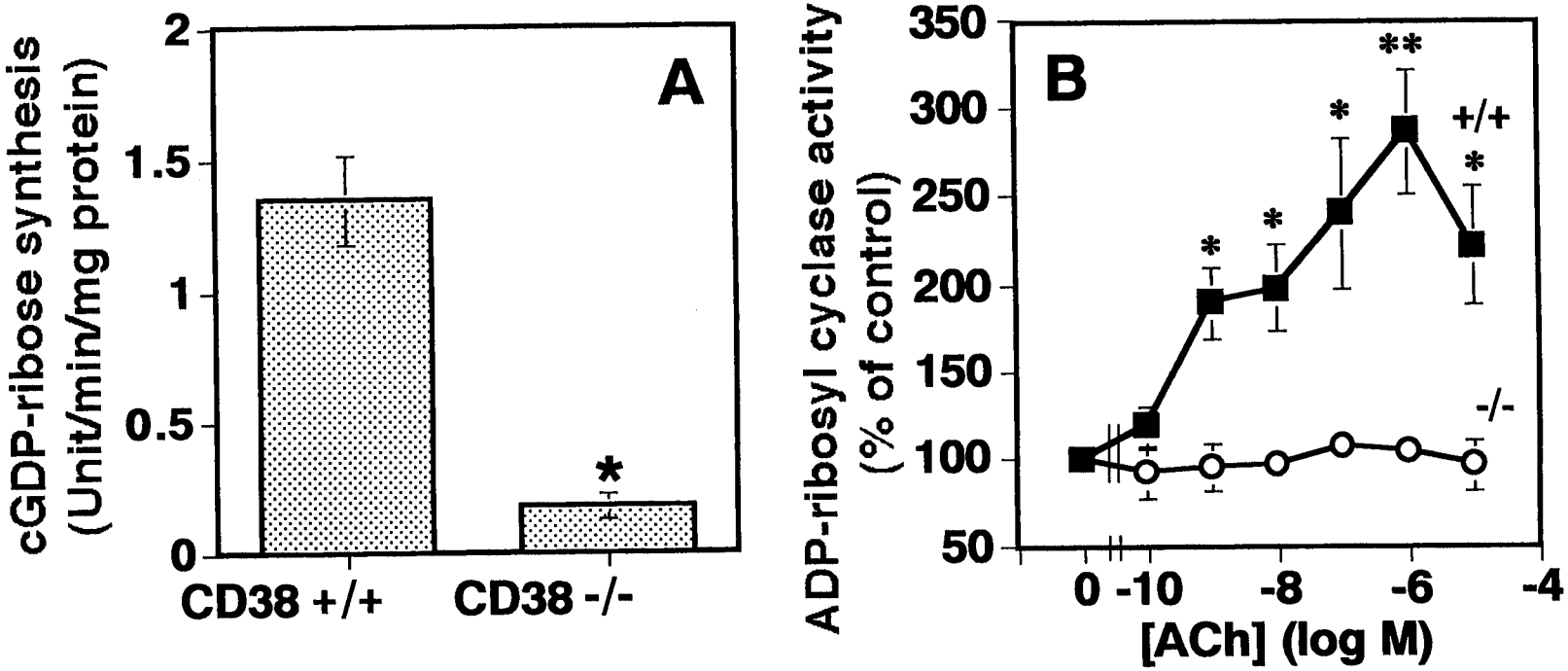
cGDP-ribose synthesis
(Unit/min/mg protein)
2
1.5
1
0.5
0
A
*
CD38 +/+
CD38 -/-
ADP-ribosyl cyclase activity
(% of control)
350
300
250
200
150
100
50
B
**
*
*
*
*
+/+
-/-
0
-10
-8
-6
-4
[ACh] (log M)

Figure 4

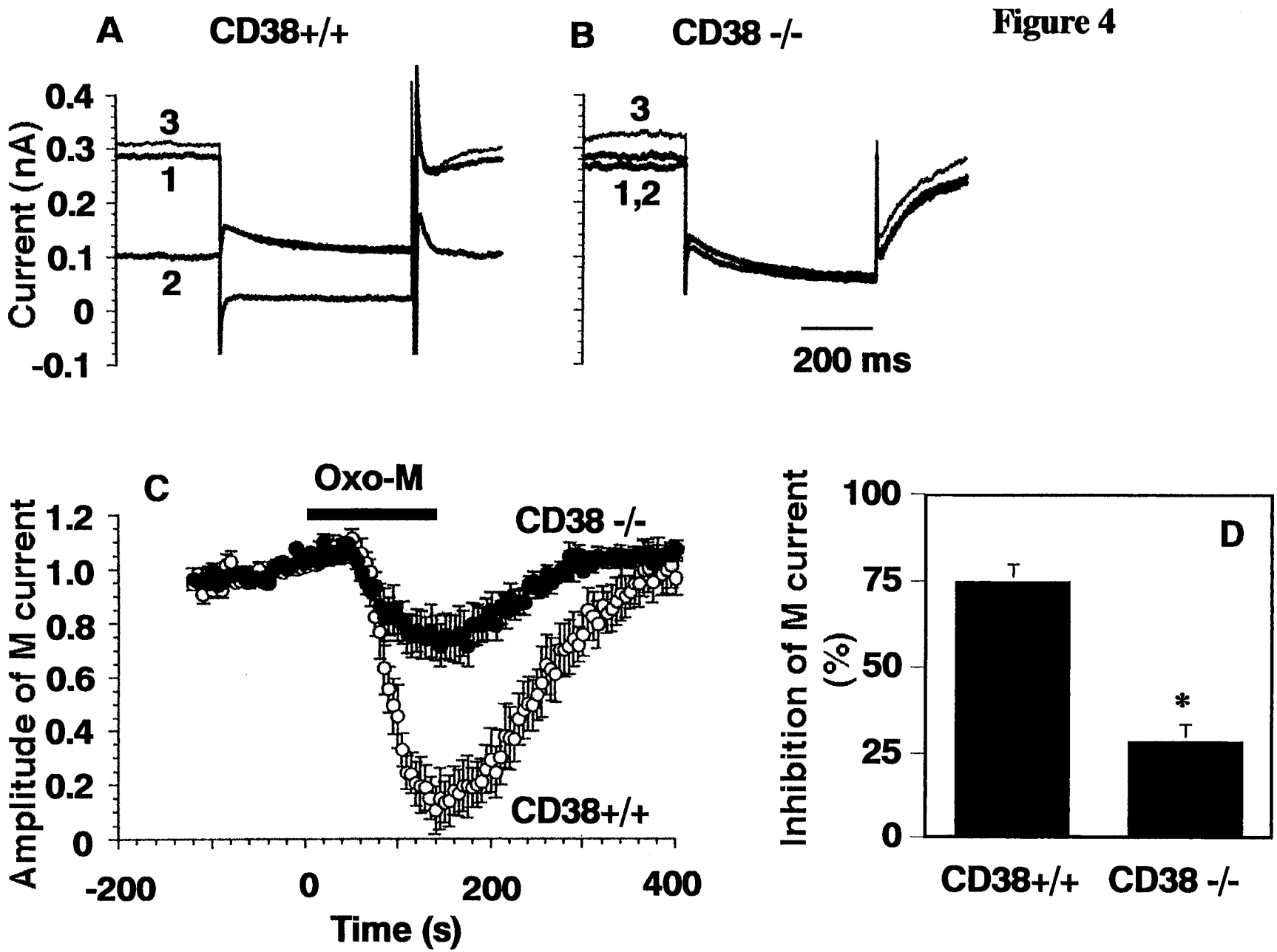
A
CD38+/+
B
CD38 -/-
Current (nA)
0.4
0.3
0.2
0.1
0
-0.1
3
1
2
3
1,2
200 ms
C
Oxo-M
CD38 -/-
CD38+/+
Amplitude of M current
1.2
1.0
0.8
0.6
0.4
0.2
0
-200
0
200
400
Time (s)
D
Inhibition of M current (%)
100
75
50
25
0
*
CD38+/+
CD38 -/-

Figure 5

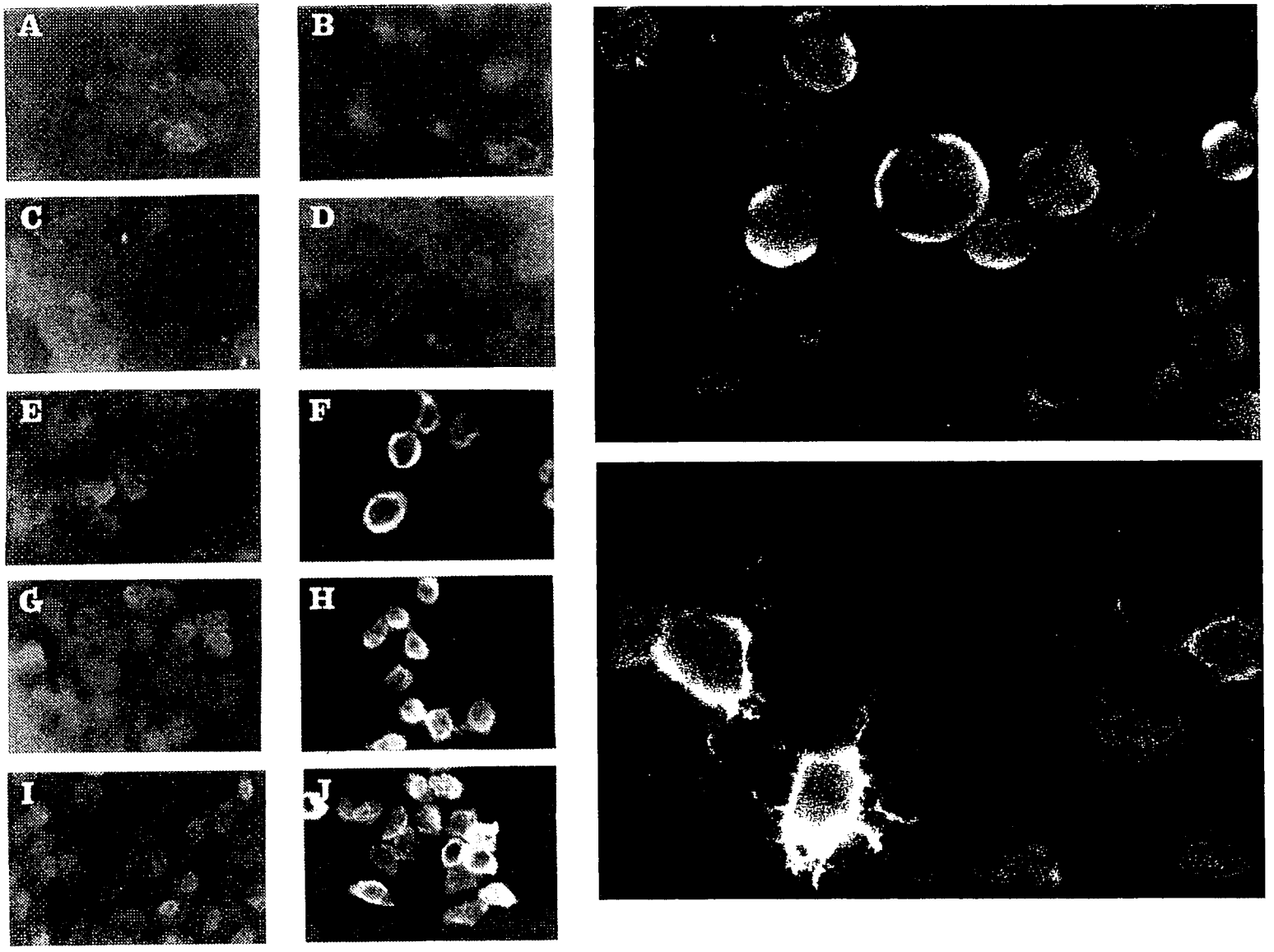

Figure 6

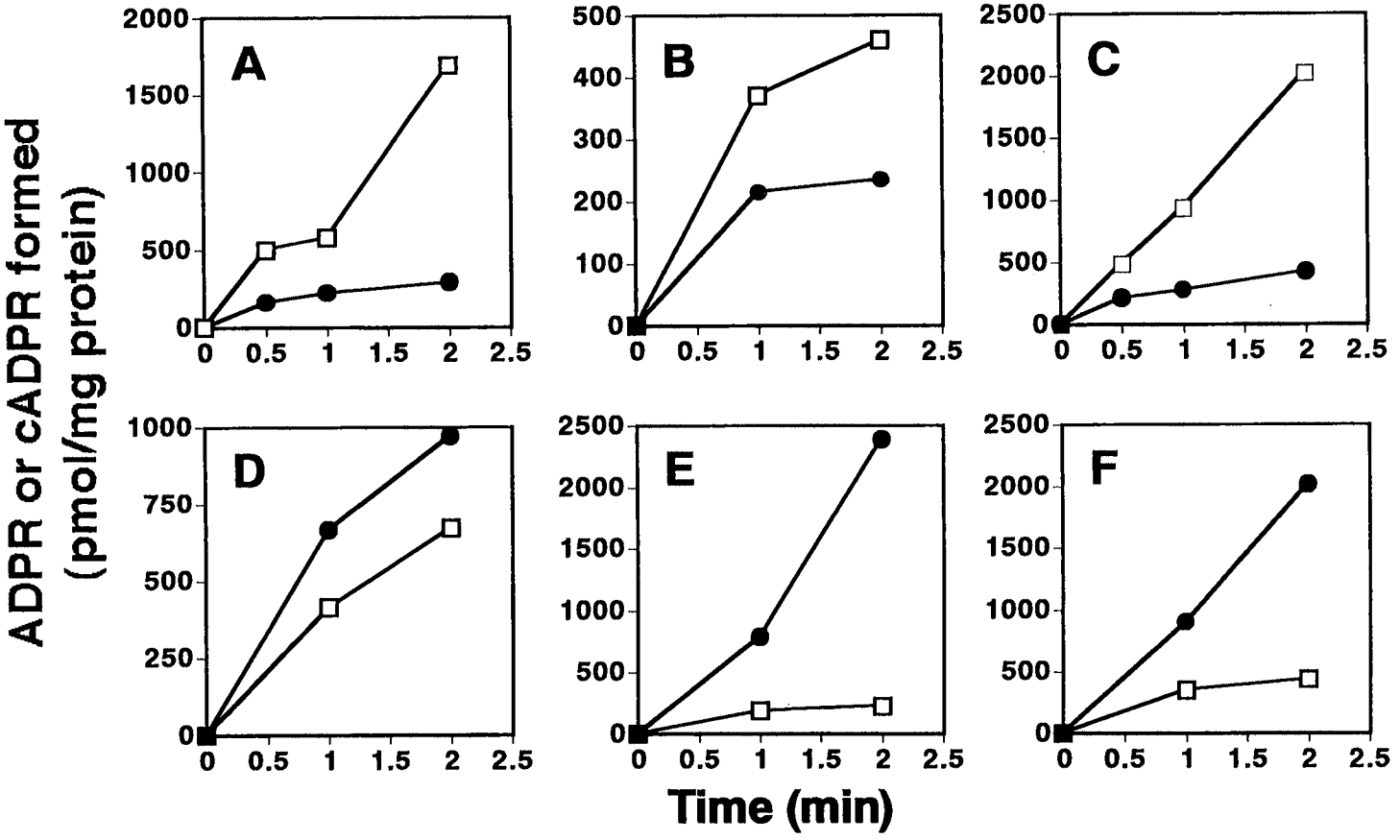
ADPR or cADPR formed
(pmol/mg protein)
A
B
C
D
E
F
Time (min)
0
0.5
1
1.5
2
2.5
2000
1500
1000
500
400
300
200
100
750
250

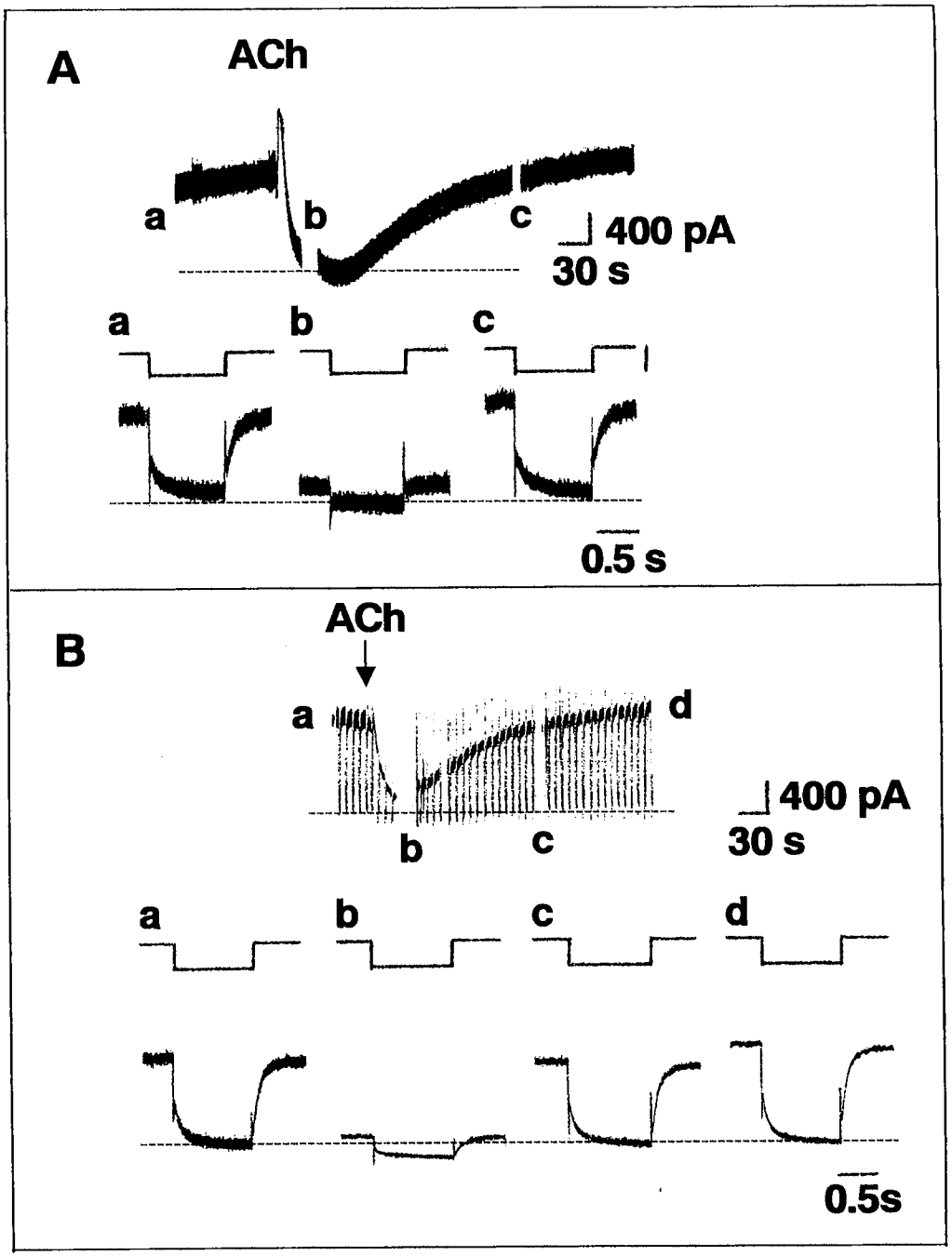

Figure 7

Figure 8

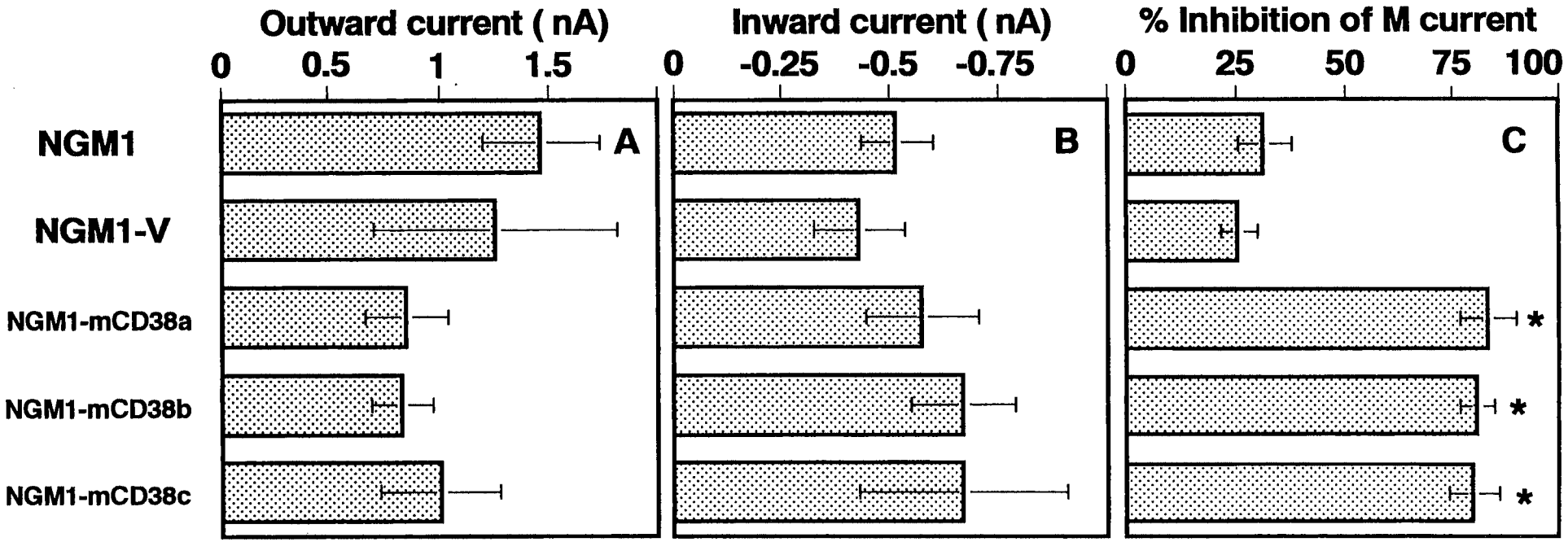
Outward current (nA)
0
0.5
1
1.5
A
Inward current (nA)
0
-0.25
-0.5
-0.75
B
% Inhibition of M current
0
25
50
75
100
C
NGM1
NGM1-V
NGM1-mCD38a
NGM1-mCD38b
NGM1-mCD38c
*
*
*

Figure 9

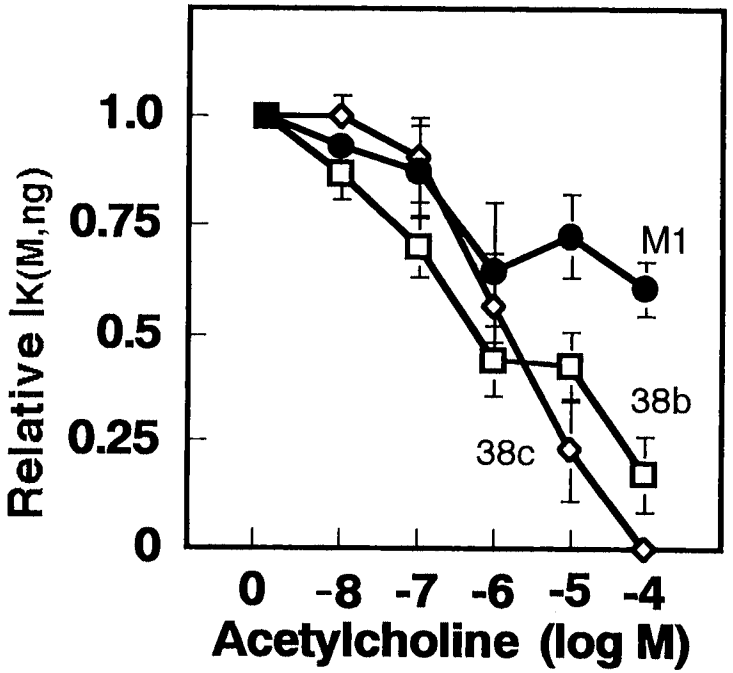
1.0
0.75
0.5
0.25
0
Relative IK(M,ng)
M1
38b
38c
0
-8
-7
-6
-5
-4
Acetylcholine (log M)

7．謝辞と展望

本研究は、京都大学中西重忠教授、大阪大学福田　淳教授、生理学研究所重本隆一教授、東北大学岡本　宏教授、九州大学野田百美助教授、ロンドン大学 DA Brown 教授・Robbins 講師等の御支援を賜った。深くお礼申し上げます。

前回の重点 B の報告においても小冊子を作り、日本中広く頒布することを取り止め、その代わり英語で総説を書くと宣言した。その結果、前回の成果を Journal of Neurochemistry 76 巻、321－331 頁（2001 年）にまとめて、より広く世界中へ発信した。今回の成果も、一流の Review 誌への掲載を行う覚悟である。